APL Photonics

TUTORIAL | FEBRUARY 25 2025

Terahertz fiber devices

Haisu Li ; Yang Cao ; Maksim Skorobogatiy ; Shaghik Atakaramians

APL Photonics 10, 021101 (2025)
https://doi.org/10.1063/5.0239310

Terahertz fiber devices

Cite as: APL Photon. 10, 021101 (2025); doi: 10.1063/5.0239310
Submitted: 18 September 2024 • Accepted: 8 February 2025 •
Published Online: 25 February 2025

Haisu Li,[1,a),b)] Yang Cao,[2,b)] Maksim Skorobogatiy,[3] and Shaghik Atakaramians[4]

AFFILIATIONS

[1] Institute of Lightwave Technology, Key Laboratory of All Optical Network & Advanced Telecommunication Network, Ministry of Education, Beijing Jiaotong University, Beijing 100044, China
[2] Center for Advanced Laser Technology, School of Electronics and Information Engineering, Hebei University of Technology, Tianjin 300401, China
[3] Department of Engineering Physics, Polytechnique Montréal, Montreal, Quebec H3C 3A7, Canada
[4] Terahertz Innovation Group, School of Electrical Engineering and Telecommunications, UNSW Sydney, Sydney, New South Wales 2052, Australia

[a)] **Author to whom correspondence should be addressed:** lihaisu@bjtu.edu.cn
[b)] H. Li and Y. Cao contributed equally to this work.

ABSTRACT

The transmission line is one of the most fundamental components for the implementation of electromagnetic systems, such as electric cables and optical fibers for microwave and optic applications, respectively. The terahertz band, sandwiched between those two well-developed spectra, is not an exception. To meet such essential demand, low-loss, flexible, wideband terahertz fibers and corresponding functional devices have witnessed a blooming interest in the past two decades, being considered as a promising candidate for building compact, robust terahertz systems thus advancing the practicality and commercialization of terahertz science and technology. In this tutorial, we will provide a concise introduction to the fundamental characteristic parameters and prevalent hosting materials of terahertz fibers. Subsequently, we will look backward over the developments of terahertz hollow-core and solid-core fibers, as well as fiber-based terahertz functional devices for communication, sensing, spectroscopy, and imaging applications. Moreover, we will discuss several remaining challenges hampering the practical utilizations of terahertz fiber devices and propose some potential solutions to current major bottlenecks.

I. INTRODUCTION

Terahertz band, generally considered to be in the frequency range over 0.1–10 THz (wavelengths 3 mm–30 μm), has been strongly featured in both fundamental and real-world applications in the past 30 years. Owing to its intriguing attributes,[1] the advancements in terahertz science and technology encompass significant strides in spectroscopy, imaging, sensing, and high-speed communications.[2–4] In particular, terahertz band offers a significantly wider spectrum bandwidth compared to the microwave, which remains largely unregulated, thus providing prospects for applications including high-speed data transmission and radar detection. In addition, due to its capability to penetrate into a variety of dielectric materials and achieve internal imaging of opaque objects, as well as low-energy characteristics that ensure harmlessness to biological tissues, the terahertz radiation offers unique advantages in non-destructive detection applications, such as security screening, quality control, and medical imaging. Furthermore, terahertz band is also rich in physical and chemical information of various materials, which enables identification of components and analysis their properties, as well as effectively differentiation of object morphology, strongly supporting the inspection tasks.

To harness the full potential of terahertz waves in the diverse applications, it is crucial to develop high-performance terahertz waveguides that can efficiently guide and transmit terahertz waves with minimal loss and distortion. There is no doubt that terahertz waveguides are intricately tied to terahertz technologies, serving as the pivotal component within terahertz systems. Their involvement enhances the versatility and efficiency of terahertz wave manipulation, enabling advanced functionalities, such as high-resolution imaging, remote sensing, and ultra-high-speed communication. Efficiently directing terahertz waves poses both a scientific challenge and a crucial determinant of terahertz technology's commercial

feasibility and practicality. Consequently, the development of high-performance terahertz waveguide has emerged as a focal point of research endeavors aimed at translating laboratory innovations into real-world terahertz applications.

At the neighborhood spectra of terahertz, i.e., the microwave and infrared field, flexible, low-loss waveguides such as radio frequency cable and optical fibers have been well-developed and standardized as one of the most fundamental components that boost commercially available, compact, and robust systems for both frequency bands. Despite the importance of waveguides for terahertz wave transmission being incontrovertible, most efforts of terahertz waveguide research still remain bound to the laboratories. One exception is the metallic waveguides but with short length (generally 1 or 2 in.),[5] rigid and cumbersome structure, which can only be applied for short-range connection between two devices using flanges. The lack of compact, flexible, long-scale waveguide with efficient end-to-end power delivery hinders terahertz wave translating from the research laboratory to the industry community or even the market.[6,7] One of the main reasons is that, most polymer materials in nature suffer from high absorption (loss tangent of order of 10^{-2} at 0.5 THz),[8] while the Ohmic losses of metal surface increase immensely compared to microwave frequency. Since dry air has relatively low absorption at the terahertz range, terahertz systems typically transmit waves in free space and manipulate them using isolated optic devices. These systems are usually bulky and demand precise alignment of every component to prevent power loss.

As the terahertz frequency range is sandwiched between the microwave and infrared, terahertz waveguides inspired from both developed fields have witnessed a surge since the late 1990s. Nowadays, the research of terahertz waveguides could be loosely classified according to their structure shapes—the planar waveguide[9–13] and fiber waveguide,[14–16] which are similar to the circuit chips of electronics and optical fibers of optical communications, respectively. Table I compares the characteristics of fiber and planar waveguides. For terahertz planar waveguides, recent advances are largely achieved based on silicon micro-fabrications and silicon-on-insulator techniques since the high-resistivity float-zone intrinsic silicon has relatively low losses at terahertz frequencies.[17] Thanks to the planar structure, both passive and active devices can be integrated inside the silicon platform.[7,9] In addition, topological photonics has been applied for terahertz planar waveguides to improve the transmission robustness at sharp corners and the on-chip device integration density.[18–20] Nevertheless, the size of terahertz planar waveguides is dominated by silicon wafers, resulting in connections limited to several centimeters or behaving as an isolated functional device. Moreover, due to the high refractive index of silicon, the single-mode, low-dispersion bandwidths of silicon waveguides are regularly narrow. In the meanwhile, waveguide tapers are most often added to couple the terahertz wave from source to the high-index waveguide—somehow holding back practical implementations.

On the other hand, terahertz fiber waveguides featuring excellent flexibility and meters-scale length tend to bring abundant opportunities for terahertz systems, thanks to the available fabrication techniques, including stack-and-drawn, additive manufacturing, and wet-chemical coating among others. However, their implementations are still restricted by their intrinsic defects together with the lack of compatible THz devices. In particular, fiber loss and coupling with other devices are two main obstacles. As mentioned earlier, due to the lack of low-loss materials, the designs of terahertz fibers always strive to improve the fractional power in the air region, so as to reduce the propagation losses. Consequently, most terahertz fibers operate as a transmission waveguide, yet the fiber-based functionalized devices are quite challenging since just a small amount of terahertz radiation could interact with the dielectric or metallic structures of fibers—otherwise the fiber devices would suffer from high losses. Similar to the planar counterpart, the

TABLE I. Comparison of characteristics between terahertz fiber and planar waveguides.

Characteristics	Fiber waveguides	Planar waveguides
Hosting material	Polymers and metals	Semiconductor
Refractive index	In the range between 1.4 and 1.8 for most polymers	~3.4 for silicon
Scale	Three-dimensional structure with a fixed cross section, up to several meters in length and cross sections of subwavelength to wavelength size	Two-dimensional structure with a thickness of several hundred micrometers, subwavelength features arranged within the plane on a centimeter-scale dimension
Transmission loss (e.g., D band)	Below 1 dB/m	Typical values of 5–10 dB/m
Mode guidance	Generally multimode	Single mode
Waveguide coupling	Lenses, waveguide taper, and antenna coupler	
Integration of devices	Solitary functionality, potential integration in all-spatial dimensions	Massive functionalities, in-plane integration
Applications	Short-to-medium range signal routing and interconnection of discrete free-space components	In-chip integration

coupling between terahertz fibers and other devices remains problematic because of the absence of a high-efficient connector. This issue may also affect the characterization of terahertz fibers. Taking one of the most popular experimental schemes, for instance, here—a terahertz time-domain spectroscopy (TDS) along with a cut-back method, the high-index lenses and metallic mirrors are used to collimate and focus free-space terahertz beam, which leads to Fabry–Pérot resonances. Meanwhile the resonant frequency (or the free spectral range) varies severely with different fiber lengths, which is unavoidable for the cut-back process. As a result, measured transmission curves of fibers, in particular fibers beyond 1 m, have oscillations in the frequency spectrum. To address the issue, horn couplers, such as the metallic cones and horns, have been employed at the ends of waveguides to increase the coupling efficiency.[21,22] Recently, horn-type adapters have been applied for terahertz fiber measurements, which provide a coupling integration between the fiber and the terahertz source/detector.[23]

In addition, terahertz fibers can also accommodate specialized designs in both cross-sectional and longitudinal directions,[24,25] for example, anisotropic core-shape fibers[26–28] and grating structures,[29,30] respectively, for various applications beyond wave transmission. Furthermore, the design of terahertz functional fiber devices suffers from challenging trade-offs between accessibility and precision of fabrication routes, as well as the absence of uniform platform. The overall size of a terahertz fiber device is typically on the submeter-level, while containing subwavelength features ranges from tens to hundreds of micrometers. This poses challenges for their experimental realization using conventional manufacturing methods, considering the state-of-the-art fine processing techniques, such as microfabrication and laser micromachining, are suitable for centimeter-scale planar structures having micro-sized features, while widely used industrial prototyping methods, such as cost-effective CNC machining[31] and additive manufacturing,[32] are more appropriate for three-dimensional structures containing millimeter-sized features. Therefore, most terahertz fiber devices currently fall into a vacuum between these two manufacturing routes. One has to choose between the compromised optical performance due to resolution limitation or the complicated post-processing requiring costly infrastructure and specialized techniques to achieve the desired functionality of terahertz devices. Furthermore, considering the diverse intrinsic defect of terahertz fibers of various material and geometries, such as weak confinement in subwavelength fiber and multi-mode operation in hollow-core fiber, there remains a notable dearth of universal terahertz fiber platform that is capable of supporting and integrating various functionalities. So far, the majority of reported terahertz fiber devices have been designed as standalone components tailored for specific applications and utilized as discrete elements in free-space systems, rather than being assembled into all-fiber circuits, despite their significant possibilities for practical applications.

To sum up, both the planar and fiber waveguides are essential components for compact, robust terahertz systems. The planar waveguide features short-scale connection with potentials of massive integration of functionalities, while bendable terahertz fibers are applicable to long-haul (up to 10 m) transmission configurations as well as middle- (several meters) and short-range (around 1 m) connections in a narrow space. Moreover, the incorporation of terahertz fiber devices, despite facing temporal challenges in experimental implementation and system integration, offers a pathway beyond some ineluctable limitations of prevailing free-space solutions. The enabled novel functionalities, such as remote sensing and imaging, as well as signal routing, has unveiled its great potential in practical applications of terahertz technology.

In the subsequent sections of this tutorial, Sec. II presents several characteristic parameters of terahertz fibers, along with the material descriptions of metals and dielectric commonly used at terahertz frequencies. Next, we categorize terahertz fibers into hollow-core, solid-core, and hybrid structures, and provide comprehensive summaries for each in Sec. III. The discussion on terahertz fiber devices and their applications in communication, sensing, and imaging is succinctly concluded in Sec. IV. In Sec. V, we address the technical challenges of terahertz fibers and highlight their opportunities and emerging trends in the near future.

II. CHARACTERISTIC PARAMETERS AND HOSTING MATERIALS FOR TERAHERTZ FIBERS

Before moving on to the details of terahertz fibers, we briefly introduce several key characteristic parameters that describe fiber performance and have significance in practice.

- ***Losses.*** Generally speaking, the transmission loss of terahertz fibers incorporates material loss (due to the material absorption of hosting materials) and confinement loss (power leakage may occur). At terahertz frequencies, common dielectrics and metals have absorptions and Ohmic loss, respectively, which are usually expressed as a frequency-dependent complex permittivity, i.e., $\dot{\varepsilon}(\omega)$, where ω is the angular frequency. For dielectrics, the real and imaginary parts of $\dot{\varepsilon}(\omega)$, or using the corresponding refractive index, i.e., $\dot{n}(\omega)$, can be extracted in terms of phase ($\phi(\omega)$) and amplitude ($\rho(\omega)$) information of terahertz TDS characterizations, respectively, which can be calculated as follows:[8,33]

$$\begin{cases} \mathrm{Re}\{\dot{n}(\omega)\} = 1 + \phi(\omega)\cdot\dfrac{c}{\omega d}, \\ \mathrm{Im}\{\dot{n}(\omega)\} = \ln\left(\dfrac{4\mathrm{Re}\{\dot{n}(\omega)\}}{\rho(\omega)\cdot(\mathrm{Re}\{\dot{n}(\omega)\}+1)^2}\right)\cdot\dfrac{c}{\omega d}, \\ \dot{\varepsilon}(\omega) = (\dot{n}(\omega))^2, \end{cases} \tag{1}$$

where d is the thickness of dielectric under test and c is the light speed in free space.

The refractive index value of dry air is almost 1, which is usually considered as the most lossless material in nature. In the field of semiconductor materials, high-resistance silicon shows a high dielectric constant of 11.7 and maintains low dispersion and material absorption within the terahertz band. Polymers can be classified into two primary categories: (1) non-polar polymers, encompassing olefin ones. According to the terahertz spectroscopic characterizations, these polymers demonstrate relatively low losses and refractive indices below 1.55 at low terahertz bands, meanwhile providing minimal dispersion. (2) Polymers containing polar bonds that lack symmetric dipole moments featuring higher refractive indices, typically exceeding 1.60. In contrast to the non-polar ones, they exhibit

abnormal dispersion characteristics (see the comparison between non-polar and polar polymers shown in Fig. 1[34]).

While away from the plasma frequency, $\dot{\varepsilon}(\omega)$ of most metals can be typically approximated using the Drude model, as expressed in Eq. (2), where ω_p and Γ are the plasma frequency and damping coefficient, respectively.[35,36] Table II shows the ω_p and Γ values for gold, silver, and aluminum at the terahertz range. From the Drude model, the conductivity of metals can be readily derived using Ohm's law,[35]

$$\dot{\varepsilon}(\omega) = 1 - \frac{\omega_p^2}{\omega^2 - j\Gamma\omega}. \tag{2}$$

TABLE II. Plasma frequency (ω_p) and damping coefficient (Γ) for gold, silver, and aluminum at the terahertz range.[35]

Metal	ω_p (s^{-1})	Γ (s^{-1})
Gold	$2\pi \cdot 2.175 \times 10^{15}$	$2\pi \cdot 0.648 \times 10^{13}$
Silver	$2\pi \cdot 2.185 \times 10^{15}$	$2\pi \cdot 0.5138 \times 10^{13}$
Aluminum	$2\pi \cdot 3.57 \times 10^{15}$	$2\pi \cdot 1.94 \times 10^{13}$

To accurately estimate the terahertz fiber loss, the frequency-dependent complex permittivity values of dielectrics and metals should be applied for the fiber model in terms of material loss. In the meanwhile, a perfectly matched layer is usually added at the

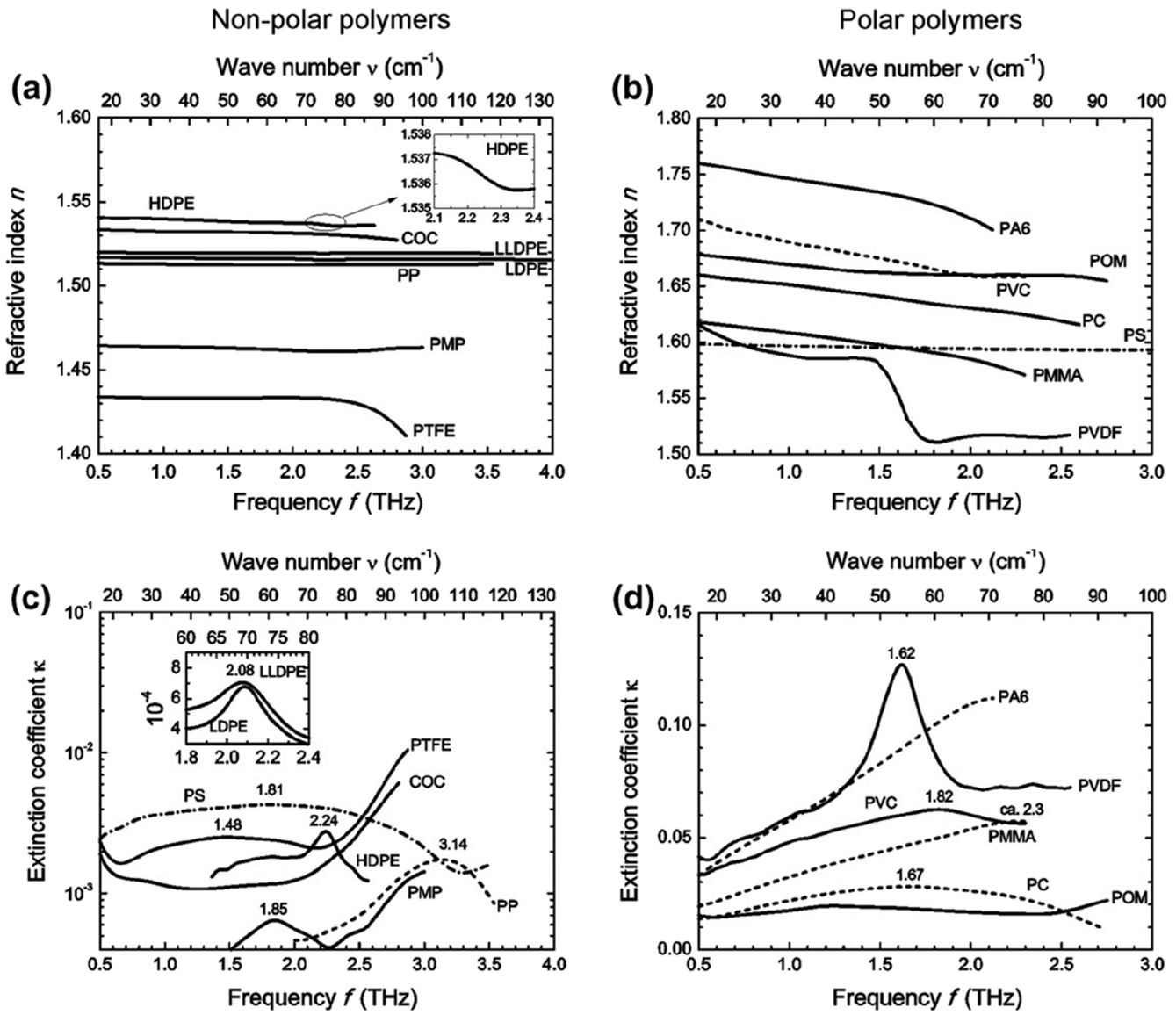

FIG. 1. Room-temperature refractive index (a) and (b) and extinction coefficient (c) and (d) of various non-polar and polar polymers, reproduced with permission from Wietzke *et al.*, J. Mol. Struct. **1006**, 41–51 (2011). Copyright 2011 Elsevier.[34]

outermost boundary of fiber cladding to evaluate the power leakage, in other words, the confinement loss. Putting the material loss and confinement loss together, the transmission loss or attenuation constant (α) of a terahertz fiber can thus be expressed as the real part of a complex propagation constant ($\dot{\gamma} = \alpha + j\beta$, where β is the phase constant). We should note here that, as a frequency range sandwiched between the microwave and infrared, the attenuation constants can be described using either the amplitude or power values[35] [see Eq. (3)], resulting in a difference of two times. Low-loss fibers are always exceedingly desirable to increase the available transmission range for terahertz systems with a known dynamic range,

$$\begin{cases} E(z) = E_0 e^{-\alpha z}, & \text{calculated in amplititude,} \\ P(z) = P_0 e^{-\alpha z}, & \text{calculated in power.} \end{cases} \tag{3}$$

- ***Flexibility.*** In the context of terahertz applications for the confined space, pliable fibers capable of maintaining high transmission around sharp corners are preferred; such a feature is usually expressed as the bending loss. In practical measurements, flexibility can be presented as the additional bending loss, via comparing the transmissions of fibers with or without bends. Bending loss is defined as the sustained loss of radiation that occurs along any curved portion of fiber and is usually related to the mode confinement performance. Impacts of bending on terahertz fiber transmission, encompassing potential losses and alterations in mode patterns, can be evaluated by the following equivalent refractive index profile of fiber, i.e., $n'(x, y)$:[37]

$$n'(x,y) = n(x,y)e^{x/R_{bend}}, \tag{4}$$

  where $n(x, y)$ represents the refractive index profile of a straight fiber and R_{bend} denotes the bending radius.
- ***Length.*** There is no doubt that one of the advantages of terahertz fiber waveguides is the long transmission range in contrast to silicon waveguides. Many state-of-the-art fabrication techniques have been devoted to realizing diverse fiber designs, which also dominate the available fiber length since the manufacturing uniformities of both cross-sectional and longitudinal directions have a significant influence on fiber performance.
- ***Operation bandwidth.*** According to Shannon–Hartley theorem, broadband spectral resource is one of the most attractive properties of terahertz band and enables higher transmission capacity of terahertz communications than that of microwave regime. Therefore, terahertz fibers with wide, low-loss transmission windows are indispensable. For a fair evaluation, both absolute and relative bandwidths should be taken into account. It is worth noting that the central frequency of a fiber device should be incorporated when using the relative bandwidth for characterizations.
- ***Structural transformability.*** In addition to the applications of terahertz fiber in wave transmission, the deformation or integration of fibers themselves, as well as the imposition of subwavelength features or additional elements on top of them, enable various functions for terahertz sensing, imaging, and communications. Therefore, the structural transformability of terahertz fiber, considering the feasibility of its theoretical design and experimental realization, is of vital importance.

  Several other attributes of terahertz fibers, which seem minor but crucial for the current development of terahertz systems, are listed in the following.
- First, group-velocity dispersion (GVD) poses challenges for terahertz fiber links, particularly as data rates and fiber lengths increase to hundreds of Gbps and meters, respectively, becoming a predominant limitation on data transmission. The calculation of GVD is expressed as follows: where β and ω are the imaginary part of the complex propagation constant and the angular frequency, respectively,[32]

$$GVD = \frac{\partial^2 \beta}{\partial \omega^2}. \tag{5}$$

  Usually, the unit of GVD is ps/THz/cm, indicating the broadening of a time-domain terahertz pulse (1 ps) after transmitting a 1 cm waveguide length at a specific frequency of 1 THz. Given that the majority of reported terahertz fibers exhibit mode distributions predominantly in the air, which is a non-dispersive dielectric medium, GVD has a relatively minor impact on fiber performance compared to insertion loss at meter scale. This observation holds true for most applications, with exceptions of long-range terahertz communication links.[38]
- Second, robust transmissions prefer a single-mode operation rather than a multimode waveguide where mode coupling and dispersion would happen. At the terahertz band, high-order modes with complex field distributions are difficult to excite since the radiation launched from present terahertz sources is usually linearly polarized. Even though terahertz fibers would support multiple modes in an oversized core to reduce transmission losses, the fundamental mode that is usually linearly polarized dominates the transmission of terahertz power.

Overall, terahertz fibers featuring a wide bandwidth with low losses, the scalability for both short- (below a meter) and long-distance (up to tens of meters) transmissions with suitable fabrications, and fantastic flexibility, are in immense demand to adapt the prompt development of terahertz systems, particularly the progress of system integration. Furthermore, we envision that innovative accessories of terahertz fibers, including special fibers required for distinctive applications, functional devices integrated on fiber platforms and, efficient connectors for terahertz fibers, will further enrich the feasible exploitations of terahertz science and technology.

III. GUIDING MECHANISMS, STRUCTURES, AND FABRICATIONS OF TERAHERTZ FIBERS

In this tutorial, we categorize terahertz fibers according to their guidance either inside a hollow-core or along solid cores. Both types of fibers propagate terahertz waves largely or partially in the air region to minimize transmission losses. Moreover, terahertz fibers with inimitable structures and guiding mechanisms, which are

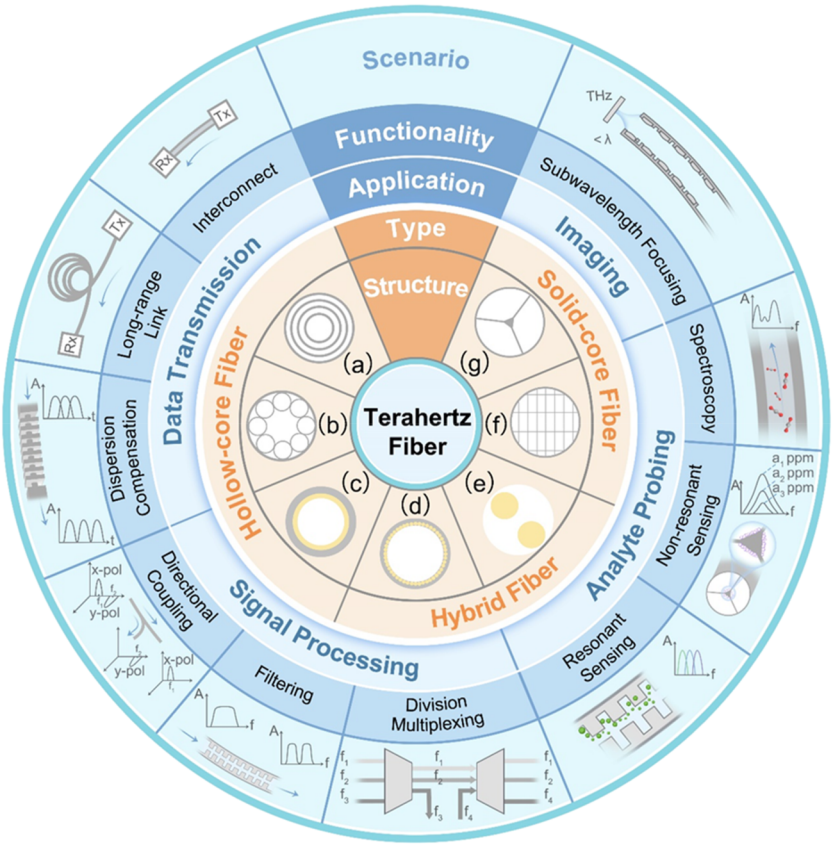

FIG. 2. Type, functionality, application, and scenario of terahertz fiber devices. Schematic diagram of the cross-sectional profile of (a) photonic bandgap Bragg fiber, (b) negative-curvature fiber, (c) metal-coated fiber, (d) hybrid cladded fiber, (e) two-wire plasmonic fiber, (f) porous fiber, and (g) suspended-core fiber.

named as the hybrid fibers in this tutorial, will also be discussed after the hollow-core and solid-core fibers. Figure 2 shows schematics of several popular terahertz fibers. Versatile functionalities can thus be integrated on terahertz fiber platforms, enriching various application scenarios.

A. Hollow-core fibers

Terahertz fibers owning an air-core require cladding designs to confine terahertz waves inside the low-index air region. In this section, we first review the photonic bandgap fibers, followed by the anti-resonant fibers, both of which are all-dielectric structures. Then, metal/dielectric-coated terahertz fibers will be presented (see their research progress in Fig. 3).

1. Photonic bandgap dielectric fibers

Photonic crystals feature photonic bandgaps where electromagnetic waves are prohibited from transmitting through.[54] Benefiting from the complete confinement, photonic crystals have been intensively applied for hollow-core optical fiber designs since the 1990s.[55] One of the major prospects is propagating the light in an air-core to reduce the transmission losses of optical fibers, substituting the conventional solid silica core where the Rayleigh scattering dominates the loss limit.[55,56] Since the early 2000s, terahertz photonic bandgap waveguides have garnered significant theoretical and experimental interest, drawing inspiration from hollow-core photonic crystal fibers. In the following content, terahertz dielectric hollow-core fibers based on Bragg and holey cladding structures (corresponding to the one- and two-dimensional photonic crystal systems, respectively) will be presented.

We start with terahertz Bragg fibers that have simpler structures and easier fabrications in contrast to the holey fibers. The Bragg fiber is generally composed of alternative high- and low-index layers in the cladding, which is basically a one-dimensional photonic crystal reflector.[57–59] A preliminary work of terahertz Bragg fibers was demonstrated in 2011.[40] Two types of fiber claddings were realized, where one employed air and polymer layers with powder particles to separate two adjacent layers, while the other was achieved using R104-grade-powder-doped and undoped polyethylene layers. Both fibers with lengths of around 22 cm and core sizes of around 6.7 mm were fabricated by rolling the polymer films. From measurements, the losses were down to 2.8 m^{-1} at 0.82 THz and 4.2 m^{-1} at 0.26 THz for the air-polymer and doped-polymer Bragg fibers, respectively. Due to an oversized air-core, both fibers are multimode, where transverse-electric (TE), transverse-magnetic (TM), and hybrid (HE and EH) modes co-exist and affect the transmission losses together. Theoretical analyses reveal that the field decay of the TM polarization dominates the loss of HE mode, thus the refractive indices of the bilayer should be appropriately selected. In addition, the Bragg fiber with high-refractive-index films can

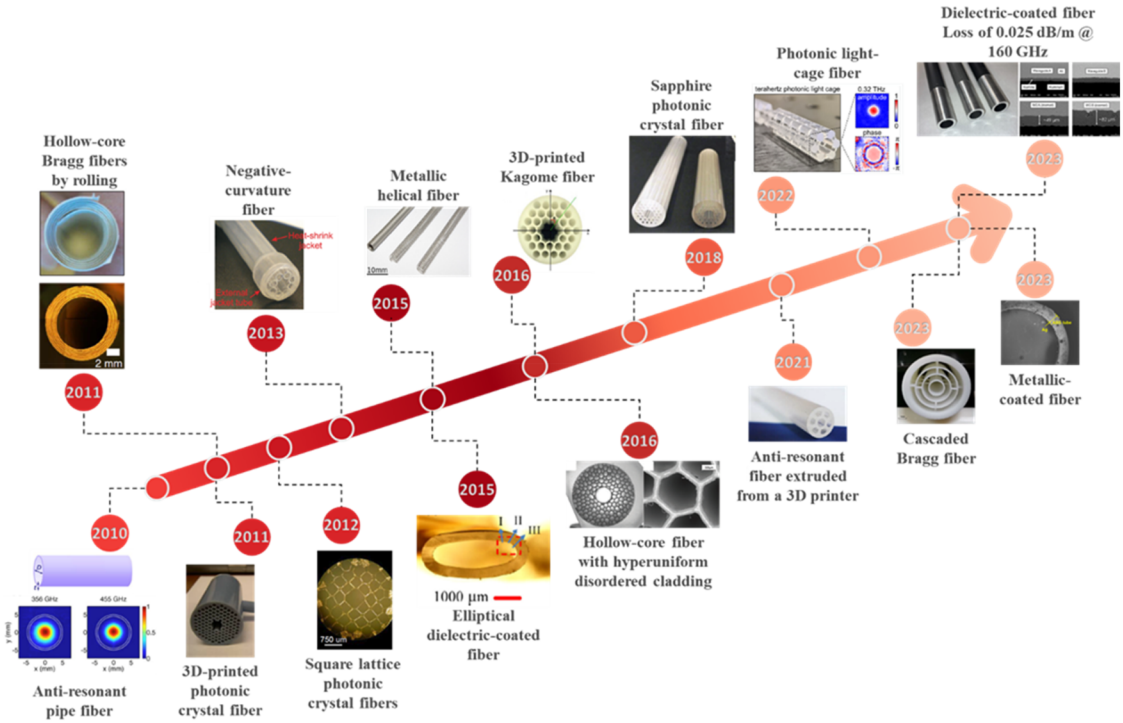

FIG. 3. Research progress on terahertz hollow-core fibers. The inset images are reproduced with permission from[39] Lai *et al.*, Opt. Lett. **34**, 3457–3459 (2009). Copyright 2009 Optical Society of America;[40] Dupuis *et al.*, J. Opt. Soc. Am. B **28**, 896–907 (2011). Copyright 2011 Optical Society of America;[41] Wu *et al.*, Opt. Express **19**, 3962–3972 (2011). Copyright 2011 Optical Society of America;[42] Setti *et al.*, Opt. Express **21**, 3388–3399 (2013). Copyright 2013 Optical Society of America;[43] Anthony *et al.*, *8th European Conference and Exhibition on Optical Communications (ECOC)*. Copyright 2012 Optical Society of America. Reproduced with permission from Optical Society of America;[44] Vogt *et al.*, Opt. Express **23**, 33359–33369 (2015). Copyright 2015 The Optical Society;[45] Tang *et al.*, Opt. Express **23**, 22587–22601 (2015). Copyright 2015 The Optical Society;[46] Yang *et al.*, Opt. Express **24**, 22454–22460 (2016). Copyright 2016 The Optical Society;[47] Skorobogatiy *et al.*, Adv. Opt. Mater. **4**, 2085–2094 (2016). Copyright 2016 John Wiley & Sons, Inc;[48] Skorobogatiy *et al.*, Adv. Opt. Mater. **6**, 1800573 (2018). Copyright 2018 John Wiley & Sons, Inc;[49] Talataisong *et al.*, Photonics Res. **9**, 1513–1521 (2021). Copyright 2021 Author(s), licensed under a Creative Commons Attribution 4.0 License;[50] Stefani *et al.*, ACS Photonics **9**, 2128–2141 (2022). Copyright 2022 American Chemical Society;[51] Bai *et al.*, Appl. Opt. **62**, 4381–4389 (2023). Copyright 2023 The Optical Society;[52] Thackston *et al.*, J. Infrared, Millimeter, Terahertz Waves **44**, 489–489 (2023). Copyright 2023 Springer Nature;[53] Liu *et al.*, IEEE Trans. Terahertz Sci. Technol. **13**, 193–199 (2023). Copyright 2023 IEEE.

be optimally designed by compromising the refractive-index contrast and material losses of bilayers.[60] Benefiting from the rapid development of additive manufacturing techniques in recent years, commercial 3D printers with resolutions down to tens of micrometers have been widely adopted for terahertz devices[60,61]—the Bragg fiber is not an exception. Both the 3D-printed terahertz Bragg fibers in Refs. 62 and 51 employ the air-dielectric bilayers in claddings. A significant challenge with these cladding structures is the lack of mechanical support between two neighboring dielectric layers, thus necessitating the incorporation of support bridges. However, the polarization of HE_{11} mode has to be perpendicular to the support bridges to maintain the bandgap effect and meanwhile minimize the additional losses contributed by the bridges. The measured losses were less than 5 dB/m within 0.246–0.276 THz for samples with the core radius of 4.681 mm and fiber lengths of up to 100 mm.[58] Moreover, to investigate the multimode operation of the aforementioned Bragg fiber, the mode transition and filtering effects were theoretically investigated, leading to an asymptotically single-mode transmission.[63] In 2023, a Bragg fiber with discontinuous support bridges in both radial and axial directions was reported. Such a complex configuration of fiber cladding was designed to prevent the influences of support bridges and was successfully realized via stereolithography 3D-printing technique.[40] The transmission losses of fabricated fiber (length of 50 mm and core radius of 3.493 mm) were 4.8 dB/m at 0.435 THz. Various compelling applications have been observed utilizing 3D-printed terahertz hollow-core Bragg fibers for powder and fluidic sensing,[64–66] which will be discussed in Sec. IV B.

Next, we proceed to the terahertz hollow-core holey fibers, which generally have periodic air holes in the cladding to achieve the two-dimensional photonic bandgap. Due to the relatively complexed structure and corresponding fabrication, terahertz holey fibers based on two-dimensional photonic crystals remained of theoretical interests[67] until an experimental demonstration using polymer jetting rapid prototyping technique in 2011.[41] The holey fiber with the central core radius of 4.2 mm was designed for operation near 105 GHz, and the measured propagation loss was 30 dB/m. After that, a terahertz holey fiber with hyper uniform disordered dielectric reflectors was 3D-printed (core diameter of 5 mm).[47] Although the air holes in

cladding are distributed disorderly, the dimensions are at a subwavelength scale (hole diameters of 113 μm vs target working wavelength around 1.3 mm), and a clear bandgap with a relative bandwidth of 15.3% at 0.29 THz is observed. The sapphire crystal, thanks to its intriguing attributes such as high refractive index and relatively low material absorption at the terahertz regime, has been introduced to the terahertz fiber waveguide community.[68] An example here is the hollow-core photonic crystal sapphire fibers that are fabricated using the shaped crystal growth technique.[48] This sapphire fiber has two rings of periodic air holes in the cladding, featuring low losses (below 10 dB/m) and flat group-velocity dispersion (0.06–1 ps/THz/cm) over a wide propagation window (0.65–1.2 THz). More importantly, the sapphire fibers hold great potential for applications in aggressive environments (the details of sensing will be presented in Sec. IV B) thanks to the high hardness and melting point of sapphire crystals. By designing the arrangement of the photonic unit cells in fiber cladding, several theoretical works report polarization-maintaining propagation in hollow-core photonic crystal fibers.. For instance, the elliptical and rectangular cores surrounded by hexagonal and square lattices have been proposed to remove the degeneracy between two orthogonally polarized modes, respectively.[28,43,69]

The aforementioned research reveals that low transmission loss is available by finely tailoring the structural design of the photonic bandgap fiber. In certain instances, improvement in the precision and reproducibility of fiber manufacturing necessitates refined fiber design and optimization of fabrication processes.

2. Anti-resonant dielectric fibers

Previously, we have reviewed the terahertz photonic bandgap dielectric fibers where the lattice constants are at the subwavelength scale. While for a bandgap waveguide with an improved lattice constant (beyond the operation wavelength), the guidance of electromagnetic waves in the hollow core is dominated by the resonant effect of the first high-index layer in cladding, rather than the lattice constant or the photonic bandgap.[70] The spectral characteristics can be analytically described by the well-known anti-resonant reflecting optical waveguide model. The mth resonant frequencies (f_m) are determined by the thickness (t) and refractive index of the innermost dielectric layer for a hollow-core waveguide (n_d), as expressed in Eq. (6),[71] where c is the light speed in a vacuum,

$$f_m = \frac{mc}{2t\sqrt{n_d^2 - 1}}. \tag{6}$$

Compared to Bragg and holey fibers, the anti-resonant fiber has a simpler structure (a thin, high-index pipe or several tubes in the cladding) and looser requirements of fabrication[72]—making it a popular candidate for terahertz hollow-core fibers in the past 15 years. Since the guiding mechanism of anti-resonant fibers is relatively convenient to achieve, we categorize relevant terahertz anti-resonant fibers as the following three structures. The first one is a simple dielectric pipe, allowing the terahertz waves to propagate inside the fiber. The second fundamental structure largely comprises a ring of capillary tubes wrapped in a large-sized tube—also called the negative-curvature fiber. For the last one, the fiber cladding is structured with the Kagome lattice, which is actually inspired by a traditional Japanese woven bamboo pattern.

The pipe fibers with a thin, smooth dielectric layer were initially investigated around the year of 2010—the pioneer of anti-resonant fibers demonstrated at terahertz bands because of their simple, commercially available structures such as Teflon air pipes or even a drinking straw.[39,71,73] These terahertz fibers generally have an oversized hollow core to prevent power absorption from the lossy dielectric materials, leading to multimode propagations while the fundamental mode (HE_{11}-like) with the lowest losses is the dominant mode.[74] The measurements show that a 3 m long pipe fiber provides low attenuation constants (below 0.5 m^{-1}, while the minimum value is 0.08 m^{-1}) over a wide transmission band of 325–525 GHz. Although the pipe fiber guides leaky modes, the losses under a 60 cm bend maintain below 0.6 m^{-1} at 420 GHz.[75] Theoretical investigations reveal that the fiber with a large core size and a thin dielectric is favorable for improving bending insensitivity. Moreover, the square- and rectangular-core pipe fibers are able to manipulate the mode polarizations and can be further applied for directional couplers by placing two of them adjacent to each other.[76] After that, several terahertz pipe fibers with modified dielectric layers are presented to broaden the transmission bandwidth since the wide terahertz spectrum is segmented by the resonant peaks. For instance, by thickening the lossy dielectric layer of the pipe fiber, the mode power attenuates fast in the cladding. Consequently, the core mode is less affected by the lossy cladding, leading to a broad bandwidth (0.3–1 THz) with low group-velocity dispersion (absolute values lower than 10 ps/THz/cm) and loss (5 m^{-1}).[37] In addition, assisted with the 3D-printing technique, pipe fibers with either a helical layer[44] or anti-reflecting structures[77] offer an extremely wide transmission window between 0.2 and 1 THz.[39,71,73]

Negative-curvature fibers have been one of the most appealing structures of the hollow-core fiber family at both optic and terahertz bands and the reasons can be twofold.[78] First, compared to the photonic bandgap fibers, the fabrication of negative-curvature fibers is much easier, meanwhile a significant improvement of uniformities for both longitudinal and cross-sectional directions of fiber samples make themselves practical in real-world applications. Second, the confinement performance of negative-curvature fibers is enhanced in contrast to pipe fibers. At terahertz frequencies, the polymer stack-and-draw technique was first adopted for negative curvature fiber manufacturing in 2013.[42,79,80] Using low-absorption Zeonex polymer, flexible hollow-core tube-lattice fibers offer low-loss (below 5 dB/m) spanning 0.25–0.35 THz,[81] which is then applied for imaging (see details in Sec. IV C).[82] The loss increase of extreme fiber bends (below 10-cm bend radii) is no higher than 1 dB/cm for thermoplastic polyurethane anti-resonant terahertz fibers.[83] Moreover, due to the multimode nature of the negative-curvature fibers (the core size is overall several wavelengths), perturbations could excite orbital angular momentum modes in terahertz hollow-core fibers. By mechanically twisting a negative-curvature fiber based on an elastic polyurethane polymer, the orbital angular momentum mode with a topological charge number of 1 has been successfully demonstrated.[84] 3D printing techniques are utilized for terahertz negative-curvature fibers, in particularly non-circular-core fibers for polarization-maintaining propagation and specially designed cladding structures to decrease transmission losses.[85–91] To separate two orthogonally polarized modes, the fiber structure just compromises a pair of dielectric slabs surrounded by a circular tube, as shown in Fig. 3, resulting in the maximum birefringence of

3.42×10^{-3} at 0.38 THz.[89] Negative-curvature fibers cladding with rotating nested semi-elliptical tubes have also been 3D-printed so as to enhance the wave confinement and in the meanwhile suppress multiple high-order modes—achieving a quasi-single mode operation.[88] Measurements show that fiber losses are down to 1 m^{-1} at 0.23 THz. Based on 3D printing, an interesting method for fast fabrication of long terahertz hollow-core fiber was proposed.[49] The fiber was extruded from a fused deposition modeling (FDM) technique, in which the printer nozzle was structured according to fiber cross-sectional designs and fabricated using a metal 3D printer. Fiber samples with lengths of up to 1 m and loss of 12 dB/m at 0.7 THz were obtained. Furthermore, terahertz light-cage fibers featuring great flexibility, or resistance to high temperatures, have been demonstrated using 3D printers.[50] Such photonic light-cage processing anti-resonant guidance popped up as a new structure to propagate electromagnetic waves inside a hollow core, which consists of a single ring of free-standing cylindrical dielectric strands of wavelength-scale diameter. The light-cage fibers, according to different polymer and ceramic materials used for 3D printing, could be applied for monitoring and sensing in high-temperature environments up to 450 °C—please refer to Sec. IV B for details.

In comparison with the terahertz pipe fibers and negative-curvature fibers, the Kagome cladding-based anti-resonant hollow-core fibers are relatively more complicated. In 2011, Kagome fibers with lengths of up to 45 mm were fabricated using the stack-and-draw approach.[92] Another terahertz Kagome fiber based on 3D printing technique offers 2 m^{-1} for 0.2–1.0 THz, and remarkably, the minimum value is about 0.2 m^{-1} at 0.75 THz.[46] Although the fiber length is limited by the 3D printer, the short sections (10 and 20 cm) can be connected to each other by using an outer tube to form a 30 cm long fiber. Such mechanical splicing between fibers provides an effective solution to achieve long-scale fiber links, for example, a 90 cm long terahertz hollow-core fiber can be built with 9 short 3D-printed segments.[93] Furthermore, similar to the twisted negative-curvature fiber supporting orbital angular momentum modes,[84] theoretical simulations have shown that high-purity orbital angular momentum modes can be guided using the high-order vector modes that existed in the aforementioned 3D-printed terahertz Kagome fibers.[94]

In summary, the ongoing exploration of anti-resonant fibers has revealed a trend toward more streamlined structures and less stringent manufacturing requirements.

3. Metal/dielectric-coated fibers

Metallic waveguides with either rectangular or circular hollow-core are commonly used as microwave transmission lines and connectors.[95] As the working frequency improves, the skin depth of metals decreases, leading to high surface resistance. In other words, the loss increases at terahertz frequencies in contrast to the microwave.[96] More importantly, the mechanical processing techniques commonly used in microwave device fabrication pose significant challenges for terahertz applications, especially at high frequencies and over long distances. Alternatively, high-precision machining (on the order of micrometers) is feasible but comes at a considerable cost. Another setback is the rigidness of metallic devices (for instance, stainless steel[97]) being unable to achieve flexible terahertz fibers. An alternative fabrication approach is an electroless, liquid-phase chemistry process to coat metals inside a polymer tube, which is initiated from the mid-infrared region,[98] resulting in a speedy progress of bendable, long-distance terahertz metal-coated fibers.

In 2004, Harrington *et al.* fabricated flexible, hollow polycarbonate terahertz fibers with interior copper coatings for broadband terahertz transmission using liquid-phase chemistry techniques. The copper-coated fibers feature losses down to the order of dB/m with fiber lengths over 1 m and air-core sizes of 2–6.3 mm.[99] We should notice that the working frequencies of those metal-coated fibers are around 2 THz, while for the dielectric counterpart, such high frequencies are generally difficult to reach—a primary bottleneck is the fabrication of microstructured claddings at shorter wavelengths.[100] In order to efficiently couple quantum cascade laser (operating at 3.2 THz) in a hollow-core fiber, low-loss (2.1–4.4 dB/m), flexible (bending losses lower than 1.2 dB) silver-coated polycarbonate fibers are employed. The measurements show that the coupling efficiencies could be higher than 80%, illustrating huge potentials for practical applications exploiting "plug-and-play" fibers in terahertz systems.[101] In recent years, the losses of metal-coated terahertz fibers are down to 0.71 dB/m at 0.3 THz,[53] accelerated by the update of fabrication techniques that ensure the geometrical precisions as well as the smoothness of the metallic layer. Most recently, experiments including tight bends (bending radius of 15 cm) and durability tests (−40 to 85 °C temperature variations over 80 h, or even below 4 K) have been carried out to investigate the practicality of metal-coated fibers.[102,103] The measurements illustrate that the metal oxidation results in an increase in transmission losses (17.11 dB/m), particularly in hot and humid environments. A possible solution is adding a thin dielectric layer, leading to minor deterioration in transmission loss (lower than 0.11 dB/m compared to as-prepared samples). Moreover, several metal-coated elliptical-core fibers are fabricated to achieve single-linear-polarization or polarization-maintaining propagations,[104–106] which have been applied for terahertz imaging (see Sec. IV C). Another terahertz hollow-core fiber worth mentioning briefly is the metallic "spring" fiber, which can be considered as the twin sister of the aforementioned dielectric helical fiber.[44] Mimicking the corrugated waveguide,[107] the metallic helical fiber has an average attenuation coefficient of 10 m^{-1} within 0.5–1 THz,[104–106] which have been applied for terahertz imaging (see Sec. IV C). Compared to its dielectric counterpart, metallic ones pose higher losses at high frequencies (over 0.7 THz).

Introducing an additional transparent, thin layer of dielectric coated inside the metallic fibers is an effective method for enhancing the reflectivity of metal mirrors.[108–110] The fiber losses can be minimized by optimizing the dielectric layer thickness (0.170 λ_e, where λ_e is determined by the operating wavelength and the dielectric constant of the layer).[52] In addition, adding a thin dielectric film on the inner surface of the metallic wall changes the boundary conditions. As a consequence, the dominant mode is a hybrid HE_{11} mode in dielectric-coated fiber rather than the TE_{11} mode for circular metallic waveguides.[111] Further theoretical studies reveal that the thickness of the dielectric film determines whether the HE_{11} mode or the transverse TE_{01} mode exhibits the lowest loss.[112] Another bonus of dielectric-coated fibers is that the oxidations of metals can be prevented,[113] as discussed in the previous paragraph. Based on the design criteria, various dielectric-coated metallic hollow-core fibers have been reported. At high frequencies, the experimentally measured losses are less than 5 dB/m in the band of 2.5–5 THz and

the values can be further reduced by improving the quality of the inner fiber layers.[114,115] For lower terahertz frequencies, a remarkable work presents that the measured transmission loss of a 1.07 m long dielectric-coated fiber is 0.025 dB/m at 160 GHz.[52] Unlike the liquid-phase deposition technique (coating the dielectric layer inside the metal walls), this fiber is first prepared using stock aluminum tubes, and then, the smooth interior of the tubes is anodized with alumina. However, the extremely low-loss fiber has lack of flexibility due to its thick aluminum walls (12.95 mm). Recently, the vacuum evaporation process has been employed for terahertz hollow-core fiber fabrication—a silver reflective layer was deposited onto the outer surface of a polypropylene tube.[116] The silver layer consists of tiny particles (about 100 nm), contributing a more uniform and smoother metal reflective layer than that could be prepared via the wet chemical method. The measured losses are 2.26 and 1.23 dB/m at 0.1 and 0.3 THz, respectively. Since the dimensional limit of vacuum evaporation equipment, the length of the fiber samples is relatively short (18.5 cm). Similar to the metal-coated fibers, terahertz elliptical-core dielectric-coated fibers have been realized to support polarization-maintaining transmissions, and the influence of dielectric layer roughness is also investigated.[45] In conclusion, through continuous research, the manufacturing process of metal/dielectric-coated fiber has undergone significant improvements, resulting in fibers with extremely low-losses and flexibility.

To sum up, the hollow-core fibers have been the most popular candidate in the terahertz waveguide field since the terahertz waves are propagated and completely confined in a low-loss air-core. Based on the well-known guiding mechanisms including 1D and 2D photonic bandgap; anti-resonant reflecting effects and metallic reflection; and modern fabrication techniques such as stack-and-draw, 3D printing, and liquid-phase deposition boost the development of hollow-core fibers. Despite the structure designs of hollow-core fiber cladding, the propagation losses are largely dominated by the material absorption of dielectrics, conductivity of metals and the air-core dimension, which is generally oversized (several wavelengths). For the fabrication end, a high uniformity of microstructured cladding that avoids local defects is preferred for dielectric hollow-core fibers, while metal/dielectric coated fibers demand a smooth interior layer to improve transmission performance. We envision that at the current stage, hollow-core fibers with relatively simple structures that allow consistent replications would play a pivotal role in real-world terahertz systems.

B. Solid-core fibers

Unlike hollow-core fibers, solid-core terahertz fibers exhibit a higher average refractive index in the core compared to that of their cladding. This inherent characteristic enables the guidance of broadband terahertz radiation along the fiber based on the well-known total internal reflection. Herein, we categorize the reported terahertz solid-core fibers into subwavelength and porous ones based on their geometries (see its research progress in Fig. 4). Despite the difference in the confinement intensity of the guided wave for each fiber design, partial power is distributed in its core region. Therefore, it

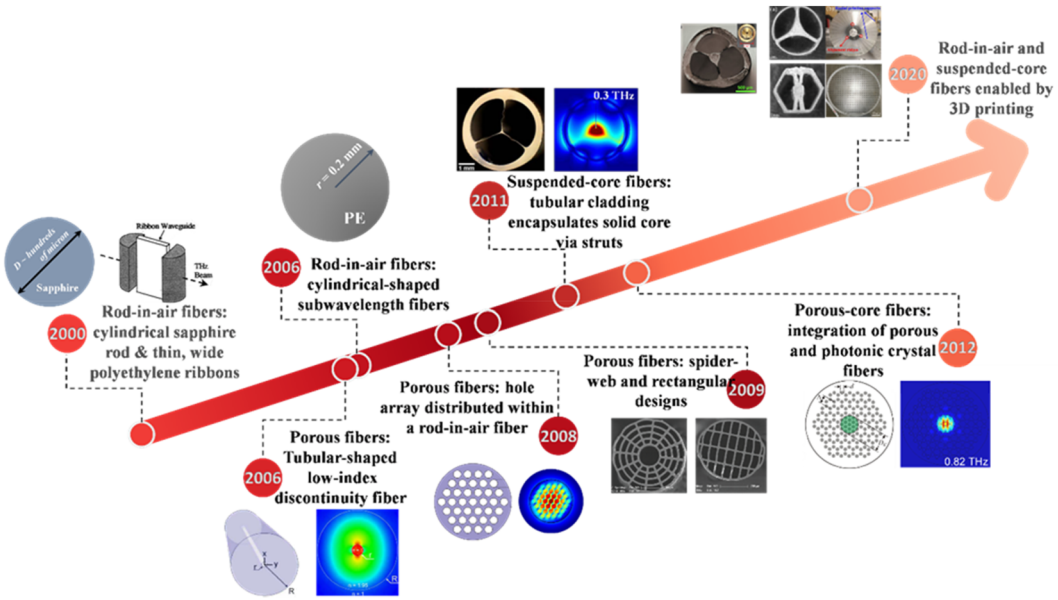

FIG. 4. Research progress on terahertz solid-core fibers. The inset images are reproduced with permission from[117] Mendis *et al.*, J. Appl. Phys. **88**, 4449–4451 (2000). Copyright 2000 AIP Publishing LLC;[118] Nagel *et al.*, Opt. Express **14**, 9944–9954 (2006). Copyright 2006 Optical Society of America;[119] Atakaramians *et al.*, Opt. Express **16**, 8845–8854 (2008). Copyright 2008 Optical Society of America;[120] Rozé *et al.*, Opt. Express **19**, 9127–9138 (2011). Copyright 2011 Optical Society of America;[121] Atakaramians *et al.*, Opt. Express **17**, 14053–14062 (2009). Copyright 2009 Optical Society of America;[122] Talataisong *et al.*, Sci. Rep. **10**, 11045 (2020). Copyright 2020 Authors, licensed under a Creative Commons Attribution 4.0 License;[123] Xu *et al.*, Sci. Rep. **12**, 4551 (2022). Copyright 2022 Authors, licensed under a Creative Commons Attribution 4.0 License;[124] Xu *et al.*, Opt. Express **31**, 12894–12911 (2023). Copyright 2023 The Optical Society;[125] Bao *et al.*, Opt. Express **20**, 29507–29517 (2012). Copyright 2012 Optical Society of America.

is crucial to utilize materials with low absorption (e.g., polyethylene, polypropylene, Teflon, and TOPAS) in the desired operational band for low-loss transmission. Although high-resistivity silicon, which exhibits remarkably low material absorption in the terahertz,[9,17] theoretically promises smaller transmission losses, challenges in mechanical processing hinder its practical applications as fibers in three-dimensional structures. In contrast, flexible polymers have been widely used to construct terahertz solid-core fiber.

1. Subwavelength dielectric-wire fibers

Inspired by the commercial silica optical fiber, a three-dimensional block structure with a high aspect ratio in isotropic lossless materials could serve as a terahertz fiber. In 2000, centimeter-long sapphire rods in circular cross section[126] and thin, wide high-density polyethylene ribbons[117] for continuous terahertz wave guidance were sub-sequentially demonstrated. To the best of our knowledge, these were the first reported works on solid-core terahertz fiber. These two fibers, which are among the simplest structures, support the HE_{11} and TM_0 modes, respectively. Despite the presence of various differences, including the cross-sectional design and refractive index contrast between the dielectric (core) and surroundings (cladding), both feature absorption coefficients less than that of the hosting materials due to their subwavelength dimension.

In 2006, cylindrical-shaped rod-in-air solid-core polyethylene fibers with centimeters-length were proposed for terahertz wave guidance within the range between 310 and 360 GHz.[127] With a core-diameter-to-wavelength ratio below 0.2, the majority of the power propagates outside the lossy core, reducing the measured transmission loss to the order of or less than 1 m^{-1}. Moreover, this fiber design allows efficient interaction with surrounding environments through end facets and side surface, thereby promising numerous applications (see discussions in Sec. IV). However, due to its mismatch with the Gaussian distributed input wave with a wavelength-scale beam spot, coupling loss exceeding 5 dB occurs at each facet.

In 2020, Nallappan *et al.* proposed meters-length polypropene subwavelength fibers operating at 128 GHz by extruding filament using a 3D printer based on FDM.[38] As a cost-effective substitute for the fiber drawing tower, rod-in-air fibers with diameters of ~0.75λ, 0.4λ, and 0.25λ (where λ is the operation wavelength) were obtained by tailoring the flow rate of extrusion and the rotation speed of the motorized spinning tool. A comparative analysis of their excitation efficiency, modal absorption loss, bending loss, and modal dispersion highlights challenges and trade-offs in the terahertz pulse propagation. In particular, the smaller fiber diameter enables smaller modal loss at the cost of enhanced extension of the electric field into the surrounding air. In addition, significant variations in the excitation efficiency, loss, and dispersion with operational frequency pose restrictions to transmitting terahertz pulse within a broadband along a fiber of a constant diameter.

It should be emphasized that the engineering challenges in handling the free-standing rod-in-air fiber necessitate the utilization of mechanical holders, such as PE films and knots at fiber ends.[38,127] However, their intrusion has an impact on the propagation and alignment of the guided wave, while sacrificing the flexibility of fibers for practical applications. In 2011, Rozé *et al.* proposed terahertz suspended-core fiber where a solid subwavelength core was supported and encapsulated by an outer tubular cladding via struts (deeply subwavelength bridges).[120] The protective cladding isolates the core-guided mode from external perturbations, ensuring minimal interaction with the surrounding environment. In addition, it serves as a natural air-tight enclosure, eliminating the need of externally purged housings. A low-density polyethylene fiber exhibiting a cladding of 5 mm outer diameter accommodating a 150 μm solid core was demonstrated for terahertz wave guidance between 280 and 480 GHz. Due to such a large aspect ratio, the electric field of the fundamental mode is highly localized in the core and rarely distributed in the lossy tubular cladding, resulting in a propagation loss of 2 m^{-1}.

It is noted that the conventional fiber drawing techniques, such as preform drilling and stacking, restrict the morphology of the fiber cross section to integral and differential multiple circles and rings of different diameters in most cases. In contrast, the advent of FDM-based 3D printing can get rid of such restrictions. On the one hand, the suspended-core fiber can be extruded from a microstructured 3D printer nozzle and directly drawn in a single-step process.[122] On the other hand, by exploiting the virtually limitless flexibility in model realization enabled by 3D printing, suspended-core fibers with relatively complicated cross section have been readily achievable. In 2022, Xu *et al.* proposed fiber design where a negative-curvature solid core suspended in tubular cladding via three supporting bridges.[123] The millimeter-scale polypropylene fibers, designed for operation at 128 GHz, were fabricated in multiple sections and assembled into meters-length ones with the assistance of their integrated outer shell and separately printed connectors. This 3D-printed modular fiber supports single-mode operation with a measured propagation loss of 4.79 dB/m. To forgo the trivial inter-sectional alignment and prevent the surge in insertion loss caused by any misalignments, the same group then demonstrated the utilization of the emerging infinite axis 3D printing to realize meters-length fibers by a single-shot process.[124] In another design, fibers in the combination of rectangular-shaped core and hexagonal-shaped cladding enable a birefringence of ~0.03–0.05 for terahertz guided waves in two orthogonal polarized modes within the range of 110–150 GHz.[124] This 3D printed fiber exhibits polarization-maintaining properties while features transmission loss of ~6.5–11 dB/m and ~6.9–13.5 dB/m for the x and y polarizations, respectively, thus opening the possibility for terahertz fiber links (see Sec. III). It is noted that the 3D printing technology transcends the constraints imposed by traditional manufacturing methods on the design of terahertz fiber, enabling realization of subwavelength fibers with intricate cross-sectional profiles.

2. Dielectric porous fibers

By incorporating a subwavelength air hole at the center of solid-core silica fiber, Nagel *et al.* proposed tubular-shaped low-index discontinuity (LID) terahertz waveguides in 2006.[118] Unlike the aforementioned pipe fibers that transfer terahertz waves through their hollow core with a diameter much larger than the wavelength,[74] the thus designed fiber supports single-mode terahertz wave transmission due to the continuity of electric flux density at the interface. Considering the refractive-index contrast at the air/dielectric interface, the discontinuity of the electrical field amplitude leads to its enhancement in the air hole. Compared to cylindrical-shaped fibers of the same dimension and hosting material, the addition of the central hole theoretically endows terahertz LID waveguide with lower transmission loss and stronger electric wave confinement. However,

the measured attenuation of 100–200 dB/m and effective permittivity of 2.5–4.0 for the terahertz guided wave in the range between 400 and 600 GHz reveals that a considerable amount of modal power is still present inside the hosting lossy material.[118]

To further push the propagating mode into air meanwhile maintaining strong modal confinement, terahertz porous fibers, in the form of a hexagonal array of subwavelength circular air holes distributing throughout rod-in-air polymer fibers, were proposed by Atakaramians *et al.*[119] and Hassani *et al.*[128,129] independently in 2008. Similar to the tubular-shaped LID fibers, the porous fibers with uniform triangular lattices can enhance electric field intensity within their air holes. An increase in the ratio of the air-hole diameter to the lattice pitch, which corresponds to thinner material veins, expels a larger fraction of modal power into the air holes inside and cladding outside of the fiber core, thus leading to a lower effective refractive index and smaller absorption loss of the fundamental mode. Compared to the subwavelength rod-in-air fiber, such porous fiber with optimal design offers larger bandwidth and lower bending loss.[128] Its overall power distribution follows a Gaussian-like envelope, allowing efficient light coupling. Using such fiber design, Dupuis *et al.* fabricated tens-of-centimeter-length porous polyethylene fibers having seven air holes in a single-layer hexagonal array in 2010.[130] The measured transmission loss of a fiber featuring an outer diameter of 775 μm and 86% porosity was less than 2 m^{-1} around 249 GHz. In 2021, Lee *et al.* demonstrated polytetrafluoroethylene two-layer-holes porous fiber with an outer diameter of 775 μm and 40% porosity.[131] This fiber exhibited a transmission loss varying from 2 to 7 m^{-1} in the frequency range between 0.1 and 0.33 THz. In addition, inspired by such porous fiber having uniform triangular lattices, Ma *et al.* proposed a graded-index fiber that incorporates air-holes with gradually increasing air-hole diameters and decreasing inter-hole separations toward the outer air cladding.[132] In comparison with the former design, the radically graded index distribution enhances modal confinement at the center of the fiber and effectively suppresses the excitation of high-order modes. Its intrinsically lower intermodal and modal group velocity dispersion results in a smaller broadening of transmitted terahertz pulses. Transmission loss varying from 2.5 to 15 m^{-1} within a frequency range between 0.3 and 1.5 THz was obtained by a polyethylene fiber having five rings in an optimal design.

Other terahertz porous fiber designs, namely, the spider-web and rectangular ones, were proposed by Atakaramians *et al.* in 2009.[121,133] Utilizing extrusion with microstructured die exit, these designs offer higher porosity compared to the hexagonal structures. Transmission loss of less than 25 m^{-1} for terahertz wave below 0.8 THz was achieved by polymethyl methacrylate (PMMA) fibers with measured porosity of 57 and 65% in these two designs, respectively. In addition, the asymmetrical transversal profile enables the rectangular porous fiber with polarization-preserving properties and a birefringence of 0.012 at 0.65 THz.

In addition, extensive research has been conducted on terahertz porous-core fibers that incorporate the concept of porous and other kinds of fibers since 2011.[134] In 2012, Bao *et al.* proposed a TOPAS porous-core photonic bandgap fiber, in which the hollow hole of a honeycomb-cladding photonic bandgap fiber is replaced by a porous core structure.[125] Compared to the hollow-core photonic bandgap fiber, such a design allows a broader bandgap and reproduction with much higher precision. Moreover, it can circumvent the unfavorable perturbation to the guided wave caused by employing extra supports, which is of necessity for applications of porous fiber. To facilitate manufacturing, air holes of consistent dimension (diameter of 165 μm) were arranged in both the fiber core and cladding regions. The measured transmission loss of 3.65 mm diameter porous-core photonic bandgap fibers within 0.78–1.02 THz is lower than the material absorption of TOPAS itself. Subsequent studies have explored further geometrical optimizations in the porous core (for example, using deeply subwavelength circular or rectangular air holes)[135–139] as well as the flexible designs for the fiber cladding (for instance, the photonic crystal fibers of versatile structures).[140–144] These advancements hold promise for improving porous-core fiber performance in theory; however, only a few have been experimentally realized.[145]

It is worth noting that achieving high porosity, which leads to low transmission loss in most scenarios, poses significant engineering challenges in fiber fabrication. In the early stages, porous fibers were fabricated using conventional methods, such as drawing stacked capillaries or a machined preform[125,129,132,146] and sol-gel casting.[130] However, these methods are time-consuming due to the requirement of pre- and post-processing procedures. Furthermore, intrinsic defects, such as the high possibility of air hole closure and severe deformation caused by active pressurization during drawing along with limitations in available sacrificial material, restricted the porous fiber design in terms of the distribution, shape, and size of subwavelength air holes, as well as its hosting materials. The extrusion with a microstructured die exit, in contrast, enables the production of porous structures with remarkable ease and precision,[131,145] while offering great flexibility in air-hole design.[121] Consequently, it has gained widespread utilization for terahertz porous fiber fabrication. Despite the broad operating bandwidth and low bending loss of porous fibers, the engineering challenges posed by their deeply subwavelength features and fiber cleaving are significant. This makes the fabrication of certain terahertz porous-core fibers, particularly those with complex transversal profiles, a formidable task." Note that the oringinal sentence is cut into two.

To sum up, most of reported terahertz solid-core fibers are based on total internal reflection. However, the free-standing cylindrical-shaped fibers suffer from either high transmission loss or susceptibility to external perturbation due to the low refractive contrast between conventional polymer and lossless air. In contrast, suspended-core fibers with a dielectric enclosure added to the air cladding can protect the guided mode in a controlled environment, thereby facilitating practical applications. Furthermore, porous fibers that incorporate subwavelength air holes in the solid core theoretically overcome this dilemma, as they confine the guided electric field mainly within these air holes through confinement by air–polymer interfaces. Nevertheless, it is worth noting that the experimental realization of numerous designs for porous fibers, especially those featuring densely and periodically arranged deeply subwavelength air holes, poses a persistent challenge in maintaining acceptable geometrical integrity.

C. Hybrid fibers

Except for the aforementioned terahertz fiber waveguides, this section presents terahertz fibers with distinctive cladding designs such as metal–dielectric hybrid structures, along with unusual

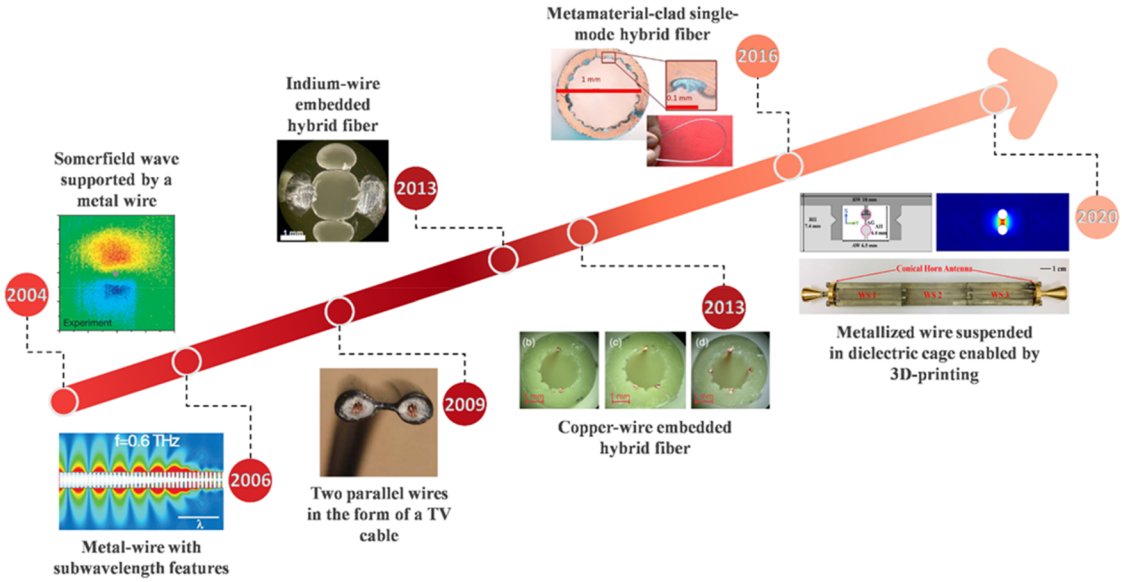

FIG. 5. Research progress on terahertz hybrid fibers. The inset images are reproduced with permission from[147] Wang and Mittleman, Nature **432**, 376–379 (2004). Copyright 2004 Springer Nature;[148] Maier *et al.*, Phys. Rev. Lett. **97**, 176805 (2006). Copyright 2006 American Physical Society;[149] Anthony *et al.*, Opt. Express **21**, 2903–2912 (2013). Copyright 2013 Optical Society of America;[150] Mbonye *et al.*, Appl. Phys. Lett. **95**, 233506 (2009). Copyright 2009 AIP Publishing LLC;[151] Atakaramians *et al.*, J. Infrared, Millimeter, Terahertz Waves **38**, 1162–1178 (2017). Copyright 2017 Springer Nature;[152] Yudasari *et al.*, Opt. Express **22**, 26042–26054 (2014). Copyright 2014 Optical Society of America;[32] Cao *et al.*, Optica **7**, 1112–1125 (2020). Copyright 2020 The Optical Society.

guidance principles according to hyperbolic metamaterials and plasmonic effects of metals (see the research progress in Fig. 5). We should note that the hollow-core metallic fibers with a coated dielectric layer discussed in Sec. III A 3 are excluded from the hybrid fibers because of the circumferential continuity of the dielectric and metal layers.

1. Hollow-core fibers based on metal-dielectric hybrid cladding

The fundamentals of hybrid cladded fibers rely on the perfect conducting for both TE and TM modes of metal wires embedded in dielectric slabs.[153] In the context of the practical realization of such hybrid structures, the fabrication approach of co-drawing polymers with indium has already been demonstrated to be a propitious option.[154] Terahertz hollow-core fibers with two and four embedded indium wires in cladding have been successfully achieved in 2013, where averaged losses of the dominant HE_{11}-like mode are 30 and 50 m^{-1} covering 0.65–0.11 THz, respectively.[149] The results illustrate that the mode diffraction losses and radiation losses in open boundary waveguides, such as parallel plates and dual wires configurations, can be eliminated in the proposed hollow-core fibers. Nevertheless, the combinations of metals and dielectrics for the co-drawing technique are quite picky, leaving a scope for improvement of fiber performance. Particularly, the commonly used metal of co-drawing, indium, has a lower conductivity (corresponding to a high Ohmic loss) compared to silver, gold, and copper. For this end, 3D-printed hollow-core fibers with copper metal wire inclusions were reported.[152] Within the frequency range from 0.4 to 1 THz, the losses are between 5 and 40 m^{-1} of a 4 mm core-diameter fiber. It is interesting that the cutoff frequencies of fibers also are unaffected by the number of metal wires surrounding the air-core. We should notice here that the aforementioned terahertz fibers cladded with metal wires have relatively large air-core diameters of 2–4 mm, resulting in a dielectric waveguide guidance. Surprisingly, by decreasing the gap distance between the two metal wires in the cladding by a factor of ~10–20, the fiber supports plasmonic guidance (for details of plasmonic fibers, please refer to Sec. II C 2).[155]

From the above-mentioned discussions of the terahertz hollow-core fibers, we can find that most fibers have large air-core sizes so as to reduce the transmission losses. Nonetheless, such an oversized fiber core beyond the working frequency usually causes multimode propagation, and as a result, modal coupling and modal dispersion become problematic. Even though the metallic circular fibers support a single TE_{11} mode operation within a wavelength-scale air-core, the corresponding single-mode bandwidth is quite narrow (i.e., 0.6–0.76 times of wavelength). To achieve an enhancement of the rigorous single-mode operation window, a terahertz hollow-core fiber with metamaterials was demonstrated in 2016.[156] The idea is inspired by the unique anisotropy of hyperbolic metamaterials—in fact a wire medium with indefinite effective permittivity tensor, which is shown in the following equation:[157–160]

$$\bar{\bar{\varepsilon}} = \varepsilon_t(\hat{\boldsymbol{x}}\hat{\boldsymbol{x}} + \hat{\boldsymbol{y}}\hat{\boldsymbol{y}}) + \varepsilon_z\hat{\boldsymbol{z}}\hat{\boldsymbol{z}}. \tag{7}$$

In Eq. (7), $\bar{\bar{\varepsilon}}$ is an effective permittivity tensor, comprising the cross-sectional and longitudinal components of $\varepsilon_t > 0$ and $\varepsilon_z < 0$, respectively.[156] In such metamaterials, the dispersion relations for

extraordinary (TM polarizations) and ordinary (TE polarizations) are strikingly different, expressed as follows:[156]

$$\begin{cases} \dfrac{k_t^2}{\varepsilon_z} + \dfrac{\beta^2}{\varepsilon_t} = k_0^2, & \text{for TM polarizations,} \\ \dfrac{k_t^2}{\varepsilon_t} + \dfrac{\beta^2}{\varepsilon_t} = k_0^2, & \text{for TE polarizations,} \end{cases} \tag{8}$$

where k_0 is the wavenumber in free space, $\beta = k_z$ is the wavevector component along the wire array, and k_t is the transverse wave vector. The aforementioned equation is exclusively applicable to the terahertz fiber incorporating anisotropic metamaterials, as shown in Fig. 6. From Eq. (8), TE waves have circular or elliptic isofrequency curves, as common dielectrics, yet the dispersion of TM waves yields hyperbolic isofrequency curves. Considering an air-core fiber waveguide with hyperbolic metamaterials described using the permittivity tensor, the isofrequency contours in k-space for an air core (blue circle) and for the hyperbolic metamaterials cladding (red dashed curve and green dashed–dotted curve for TE and TM waves, respectively) are shown in Fig. 6(a). Consequently, only TM waves can be found in the core—in other words, the transmission of TM waves is prohibited in the metamaterial cladding. The orange dotted curve in Fig. 6(a) indicates an example of a possible β value for TM modes. On the contrary, TE-polarized modes transmit into the metamaterials. Therefore, analytical modes of the metamaterial-clad fibers clearly reveal the striking TM-only guidance. Moreover, Fig. 6(b) compares the modal cutoffs of the metamaterial-clad fiber, metallic fiber, and hollow dielectric fiber as a function of normalized frequency. This illustrates that the proposed waveguide can support a strong wavelength scale TM mode confinement with a considerably larger single-mode bandwidth than metallic waveguides. Further numerical simulations suggest that a much more practical, simple fiber design consisting of a single layer of subwavelength metal wires (in contrast to a cladding entirely filled with metal wires[161]) is adequate to support TM-only propagations. Figure 6(c) presents the simulated electric field distributions and electric vectors of TM_1 and TE_1 modes of the fiber with a single layer of metallic wires. It should be noted here that the mode names, TM_1 and TE_1, given here are only applied for the metamaterial-clad fiber, representing the first order mode for TM and TE polarizations, respectively.

Benefiting from the drawn-metamaterial fabrication process,[151,162] the metamaterial-clad fiber was successfully realized, the cladding of which was constructed by a ring of indium wires embedded in a Zeonex polymer host.[163] First, for experiments, transmission measurements present a large transmittance ratio (over 15 dB) between the TM_1 and TE_1 modes, illustrating the unique optical response of wire-type hyperbolic metamaterials (reflecting TM waves but transmitting TE waves). Second, the near-field imaging of the fiber output end agrees well with the simulations, further confirming the single TM_1 mode guidance in the metamaterial-clad fiber. In short, the fabricated fiber sample supports a strict single-mode bandwidth of TM_1 mode ranging from 0.31 to 0.44 THz in a wavelength-scale air-core (diameter of 0.88 mm). In addition, the surface-plasmon–polariton-like modes are experimentally observed at the core-cladding interface. By replacing some subwavelength metallic wires with air-holes, which are vertically symmetric in the cladding (for example, along the y axis), only an x-polarized TM_2 mode exists and propagates over 0.36–0.46 THz. The quasi-linearly polarized TM_2 mode has a better coupling efficiency in contrast to that of TM_1 mode with a radially polarized mode pattern. We note that the transmission losses (beyond 28 dB/m from simulations) of metamaterial-clad fibers are higher compared to modern hollow-core terahertz, which can be attributed to the reduced core sizes. One potential approach to decrease the loss is using other metals, such as aluminum, for subwavelength wires.[164] Furthermore, an anti-resonant terahertz fiber with metamaterial cladding was proposed in 2020.[165] Simulations of the hybrid fiber show that broadband terahertz radiation can be guided with six times lower loss in such hollow-core fibers with metallic inclusions, compared to tube lattice fiber. In summary, metal dielectric hybrid cladding fiber shows huge potentials for mode manipulation. However, we should note that the transmission losses should be further decreased.

2. Plasmonic fibers based on metallic wires

The interaction between photon radiation and collective oscillation of free electrons in metal offers another solution for broadband single-mode waveguiding in metal/dielectric hybrid structure,

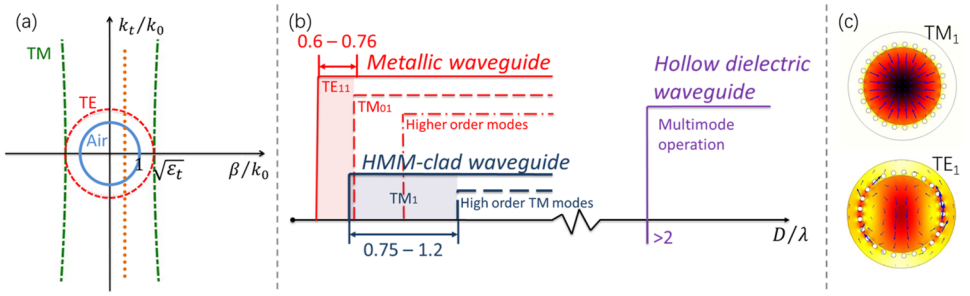

FIG. 6. (a) Isofrequency contours for waves in air (blue solid circle) and hyperbolic metamaterials cladding (TE wave, red dashed circle; TM wave, green dashed–dotted hyperbola). The orange dotted line shows an example of β value corresponding to TM-only guidance. (b) Modal cutoffs of the proposed HMM-clad waveguide (blue), metallic waveguide (red), and hollow dielectric waveguide (violet) as a function of normalized frequency. (c) Electric fields and vectors (blue arrows) of the TM_1 and TE_1 modes. The inset images are reproduced with permission from[156] Li *et al.*, Optica **3**, 941–947 (2016). Copyright 2016 The Optical Society.

the schematic of which is shown in Fig. 7(a), i.e., plasmonic waveguide. The surface plasmon–polariton (SPP) wave manifests itself as a localized field exponentially decaying from the interface and propagating along the surface. The perfect conductor-like behavior of metals effectively expels the modal electric field into the adjacent dielectric region, thus minimizing the contribution of metal ohmic loss to the plasmon propagation loss. Therefore, the guidance properties are highly reliant on the characteristics of the dielectric, which is lossless air typically. In contrast to the subwavelength plasmon size and micrometers propagation length within the visible-near-infrared spectral range, the penetration depth into dielectric $L_z{}^1$ and theoretical propagation length of terahertz plasmon $L_x{}^{pl}$ [see Eq. (9) for SPP wave in air] are on the order of centimeters and meters, respectively.[35] The subsequent equations are exclusively for the terahertz SPP wave supported by metal and propagating within air,[35]

$$\begin{cases} L_x^{pl} \approx \dfrac{\lambda_y}{n_{air}^3 \pi} \dfrac{\lambda^2}{\lambda_p^2}, \\ L_z^1 \approx \dfrac{\lambda_y^{1/2}}{\sqrt{2} n_{air}^2 \pi} \dfrac{\lambda^{3/2}}{\lambda_p}. \end{cases} \tag{9}$$

Building upon this concept, the terahertz plasmonic waveguides in one of the simplest two- and three-dimensional structures, i.e., planar metal substrate and bare metal wire in air, were proposed by Jeon and Grischkowsky and Wang and Mittleman in 2006[166] and 2004,[147] respectively. According to the wave vector of the terahertz SPP wave derived from Maxwell's equation, both of them support dispersion-less propagation of broadband terahertz wave with velocities approaching the speed of light in air [see Fig. 7(b) for their dispersion relations]. Different from the former waveguide, the terahertz SPP wave supported by a bare metal wire, which is known as the terahertz Sommerfeld wave, exhibits a radically polarized field with relatively stronger modal confinement due to its cylindrical symmetry. In addition, a distinctive dispersive trend was observed for subwavelength metal wires where phase velocity drops slightly as the frequency decreases. Such deviation from linear light lines becomes increasingly evident by reducing the wire diameter.[167]

The terahertz Sommerfeld wave exhibited low transmission loss and GVD when transmitted through stainless steel with a diameter of 0.9 mm and copper wires with diameters of 0.52 mm in experiments conducted around 2004.[147,168] Nevertheless, the weakly confined nature renders Sommerfeld wave susceptible to wire curvature and interruption.[168,169] Even slight macro-bending and small inter-wire gap with/without angular offset can result in substantial insertion loss, thus restricting the practical application of the bare metal wire. Modifications including depositing a dielectric film and imposing periodical deeply subwavelength grooves on single bare metal wires have been proposed to enhance the modal field confinement.

For the former design, which has been exploited for application in sensing and spectroscopy (see Sec. IV B for detailed implementation), the incorporation of a dielectric film with a thickness on the order of tens of micrometers can induce spatial collapse and a frequency-dependent complex effective refractive index of the terahertz SPP wave. Unlike the bare metal wire, as larger power fraction transports in the coating at higher operational frequency, terahertz pulse suffers from serious distortion when propagating over short distances and even nondispersive dielectric are adopted.[170] For the later design, which is inspired by the Goubau line,[171] the modal confinement primarily relies on corrugations on wire surface rather than the finite conductivity of metal.[148] Due to its optical characteristics resembling those of SPP waves, the supported surface wave is also known as spoof SPP. By adjusting the textured surface geometry, including the groove depth, duty ratio of rings, and period length, one can tailor its dispersion diagram and modal electric field with flexibility,[172] as the dispersion relations shown in Fig. 7(b). However, experimental demonstration remains challenging, partially due to the engineering difficulty in reproducing the three-dimensional periodical features on metal wires.

The above-mentioned single metal wire waveguiding solutions are known to confront with a trade-off between modal localization and loss. In addition, their supported radially polarized wave differs from the linearly polarized terahertz radiation emitted by the majority of terahertz sources. Consequently, inefficient coupling poses challenges in applications. To address these inherent

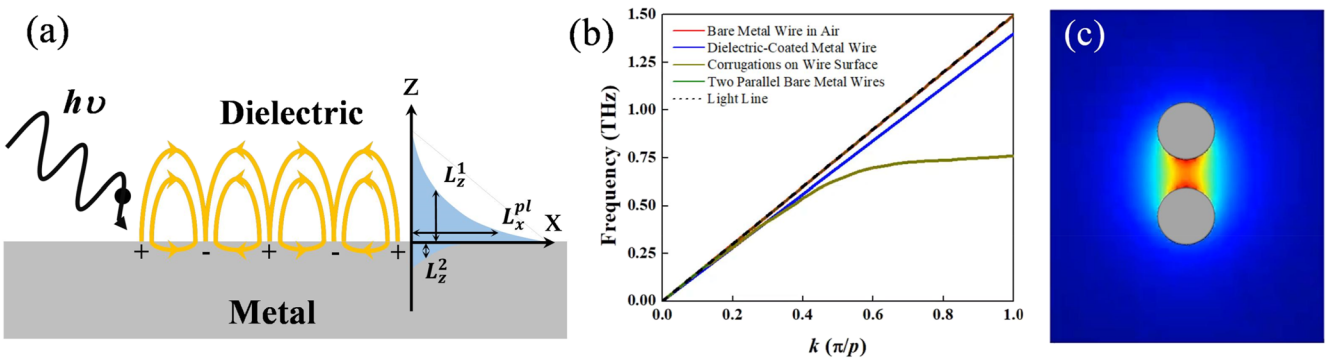

FIG. 7. (a) Schematic diagram of the excitation and propagation of the terahertz SPP wave. (b) Dispersion relations of terahertz plasmonic fibers in a single metallic wire in the first Brillouin zone. (c) Transverse modal electric field amplitude distribution of the terahertz SPP wave supported by a stand-alone two-wire waveguide.

defects, a terahertz waveguiding solution in two parallel conductive wires, which was adapted from the twin-lead cable for RF signal transmission, was proposed by Mbonye *et al.* in 2009.[150] With an electric field predominately confined in the dielectric gap and polarization parallel to a line connecting the wire axes [see Fig. 7(c) for its transverse amplitude distribution], the fundamental TEM mode exhibits small transmission and bending loss, as well as negligible GVD, while also enables efficient excitation using standard terahertz photoconductive antennas.[173,174] Moreover, compared to the single-wire configuration, the combination of higher structural flexibility and more controllable modal field distribution endows the two-wire waveguide with great tunability in terahertz wave guidance.[175–177] It has served as a versatile platform for terahertz signal manipulation (see Sec. IV A for discussion in applications).

It is worth noting that the practical implementation of standing-alone two-wire waveguides encounters challenges arising from the exposed air gap and engineering difficulties in aligning wires. To leverage their outstanding terahertz properties while meanwhile ensuring structural stability, Markov *et al.* demonstrated a simple waveguide design where two metal wires were protected with porous plastic foam and stretched using mechanical holders. It was followed by hybrid designs realized by placing metal wires into the microstructured cladding of a hollow-core fiber.[15,178,179] However, the existence of lossy dielectric in wire separation and the cumbersome wire-fixing holders still have a negative effect on the guided terahertz SPP wave in a negative manner.

Considering the tens-of-nanometers penetration depth of terahertz wave into metal, optically thick metallic coating on 3D-printed polymer surfaces, which is readily achievable by sputtering and wet chemistry deposition,[180,181] performs comparably with components machined from bulk metals for terahertz SPP wave guidance. Cao *et al.* proposed a micro-encapsulate two-wire waveguide design where two metalized photosensitive cylinders are suspended in dry air and encapsulated by a dielectric cage.[32] Such design circumvents the intrusion of leaky materials into the air gap between wires, thus inheriting most advantages from free-standing waveguides that are applicable only in theoretical analysis. Meanwhile, it features exceptional structural robustness and flexibility, as well as a unique modular nature, thereby enabling the construction of highly reconfigurable plasmonic circuits of complex functionalities (see Sec. IV for implementations in detail).

D. Discussions

The aforementioned three types of terahertz fibers, hollow-core fibers, solid-core fibers, and hybrid fibers, each exhibit distinct characteristics. Hollow-core fibers are highly favored for their low-loss transmission properties, which can be attributed to the concentrated modal field distribution within the dry air inside fiber core. Solid-core fibers, due to the strong interaction between terahertz waves and hosting materials, are particularly suitable for the development of functional devices. Hybrid fibers, integrated of both dielectric and metal, show significant advantages in mode manipulation and signal processing applications. Several key attributes of these fibers are summarized in Table III.

Researchers at the community of terahertz fiber waveguides may always meet the challenge that the fiber attributes of fabricated samples remain a scope for improvement compared to the theoretical values, particularly the transmission bandwidth and loss. This is largely because of the fabrication imperfections and limitation—considering the current situation of the lack of low-loss materials at the terahertz regime. From the above-mentioned review of the current development of terahertz fiber waveguides, we briefly discuss three popular fabrication techniques, including 3D printing, fiber drawing, and metal/dielectric coating. 3D printing has been the most attractive approach for rapid, cost-efficient realizations of terahertz fiber and devices that have relatively complex structures or non-circular core shapes, such as hollow-core fibers with photonic claddings and polarization-sensitive fiber devices. Photopolymer resins and thermoplastic, for example, acrylonitrile-butadiene-styrene and polylactic acid, are most commonly used dielectrics for fabrications of terahertz fibers, which can be further coated with metals to achieve metallic or metallic/dielectric hybrid structures. However, for terahertz fiber devices, the corresponding subwavelength structures may be down to a scale of tens of micrometers, which are almost approaching the resolutions of commercial 3D printers, resulting in fabrication errors of geometrical parameters. Moreover, we would comment that the flexibility of 3D-printed fiber needs to be enhanced as the current 3D-printable materials are usually stiff. For more details, readers are suggested to refer to Refs. 16 and 182 among others. Fiber drawing at the terahertz band aims to achieve long-scale, dielectric-based fibers. In general, available materials include PMMA and cyclic-olefin-copolymer

TABLE III. Comparison between different types of terahertz fibers.

Fiber type		Transmission loss (dB/m)	Bandwidth (THz)	Bendability	Dispersion (ps/THz/cm)	Fabrication	Additional functions
Hollow-core fibers	Bandgap[51]	<5	0.382–0.45	···	···	Stereolithography	···
	Pipe[37]	21.7–217	0.3–1	Yes	−10 to 10	Commercial PMMA tube	Data transmission
	Negative-curvature[49]	12	0.4–1.5	···	···	Fused deposition modeling	Data transmission
	Kagome[94]	1.6–8.2	0.2–0.9	···	−0.5 to 0.5	3D printing	···
	Metal coating[53]	0.71	0.2–1.0	Yes	···	Chemical deposition	Confocal imaging
	Dielectric coating[52]	0.025	0.1–0.5	···	···	Anodizing	Data transmission
Solid-core fibers	Suspended core[123]	4.79	0.11–0.15	Yes	−2 to 4	Fused deposition modeling	Data transmission; imaging
	Subwavelength[38]	0.62	0.2–0.6	Yes	0–8	Fused deposition modeling	Data transmission
	Porous[130]	<8.69	0.16–0.31	Yes	···	Sacrificial polymer technique;	···
Hybrid fibers	Plasmonic[32]	26	0.11–0.17	Yes	1–2	Stereolithography	Signal processing
	Metamaterials[156]	28	0.31–0.44	Yes	···	Fiber-drawing	···

(COC, and the trade names of that are Zeonex and TOPAS among others). To improve fabrication accuracy in both cross-sectional and longitudinal directions, the drawing parameters, such as the temperature, speed, and pressure, should be carefully controlled. Nonetheless, the metal/dielectric co-drawn technique is especially applicable for the intriguing terahertz metamaterial fiber devices, as we have presented in Sec. III C 1. Terahertz metal/dielectric coated fibers have been the record of transmission losses, which can be fabricated using the wet chemical deposition method. However, the experimental losses are still higher than the theoretical values, which can be attributed to the fabrication imperfections of compactness of metallic film and non-uniformities of the metal/dielectric-coated layer, particularly for the fibers up to several meters.[45] Therefore, similar to the fiber drawing method, the liquid-phase chemistry process needs to be precisely supervised. In order to achieve high-quality coating of metal layers, other fabrication techniques (such as the electroplating approach and vacuum evaporation process) are worth exploring, as the anodizing method has been demonstrated for dielectric-coated metallic fibers to offer the lowest propagation losses, to the best of our knowledge.[52]

In the context of fiber fabrications, drawing and extrusion processes are beneficial to the manufacture of long-distance fibers but confront certain challenges in achieving uniformity in both the transverse and longitudinal directions of fibers. In contrast, 3D printing technology demonstrates superior performance in terms of precision and uniformity, although it is limited in the fiber length. In addition to these fabrication techniques, the preparation of metal/dielectric hybrid fibers also involves metallization processes, offering new possibilities for performance optimization and functional expansion of terahertz fibers. Last but not the least, the fabrication cost, which plays a significant role for the commercialization progress of terahertz fibers, should be balanced with accuracy.

IV. TERAHERTZ FIBER DEVICES AND THEIR APPLICATIONS

The development of terahertz fiber-integrated devices with versatile functionalities has significantly enriched applications ranging from microscopic material science to macroscopic information systems. Figure 8 presents a conceptual diagram that encompasses terahertz fiber-based applications in communication, sensing, spectroscopy, and imaging. For terahertz communications, flexible terahertz fibers enable long- and short-range data transmissions in environments challenging for wireless communications, including compact interiors of satellites and adverse weather conditions. Signal processing sub-systems, such as dispersion compensation, filtering, directional routing, and division multiplexing, have been demonstrated on terahertz fiber platforms. In addition, as a frequency range lying between the mature microwave and infrared waves, terahertz waves are expected to play a critical role in reducing power consumption of diverse optoelectronic systems by forgoing the need for conversion between optical and electronic signals. A potential scenario—data center, where terahertz fibers could meet the requirement of high-speed data connections between electronic storage and processing units, is shown in Fig. 8. Moreover, in the next-generation wireless communication systems, conversion of signals from optical backbone networks to terahertz bands are readily achievable, owing to the successful development of photodiodes in recent years. In addition, in the field of terahertz integrated sensing and communication, a series of exciting functionalities are available through the involvement of terahertz fiber devices, such as

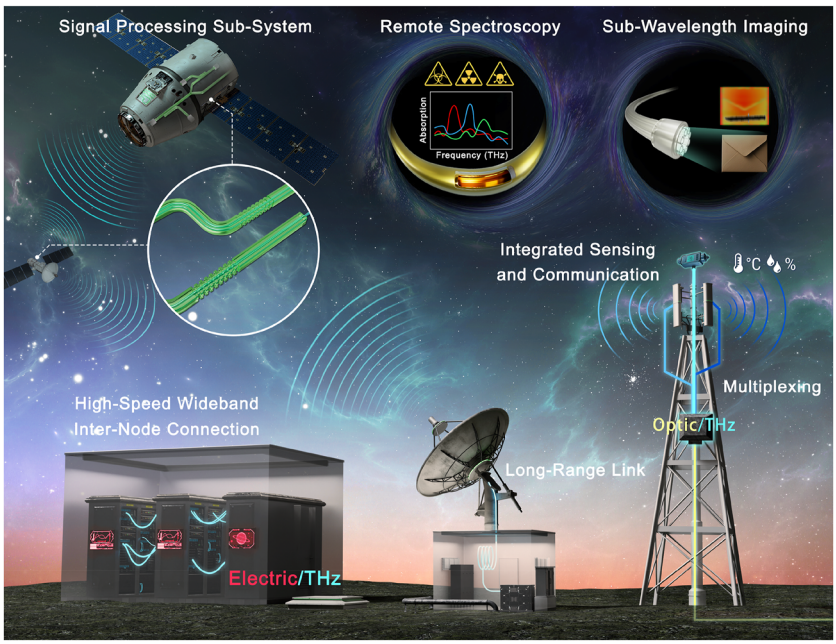

FIG. 8. Schematic diagram of an integrated terahertz system encompassing terahertz fiber devices.

environmental monitoring of humidity and temperature. In the context of spectroscopy and imaging, flexible terahertz fiber devices, benefiting from the long-distance, stable transmission features, are particularly suitable for detecting remote targets. Furthermore, subwavelength focusing is also achievable using terahertz fibers, as illustrated in the right-top panel of Fig. 8.

A. Communications

Having a broad unregulated spectrum, the terahertz band offers substantial bandwidth resources to address spectrum scarcity. The advancing terahertz wireless communication has been envisioned as the next frontier in wireless communications to cater to the escalating demand for ultra-high-speed data transmission. In most studies, the modulated terahertz carrier waves are generated and received by terahertz transceivers, and their propagation is aided by discrete beam steering and focusing devices in free space. However, some fundamental signal processing functionalities remain unachievable in the terahertz band due to the lack of mature terahertz signal manipulation technologies or engineering challenges associated with their implementations. In addition, in certain scenarios, the performance and stability of wireless links could be significantly compromised due to inherent defects of terahertz radiation (for instance, the high directionality and strong water absorption). Instead, drawing inspiration from silica optical fibers, the incorporation of terahertz fiber devices can provide new perspectives for terahertz communication networks.[4,183] In this section, we briefly summarize the application and potential of the above-mentioned classic terahertz fibers for data transmission and signal processing.

In terms of data transmission, to achieve a high data rate at acceptable bit-error-rates (BERs), one usually needs to ensure low insertion loss and distortion of broadband terahertz pulses, which imposes stringent thresholds on the terahertz fiber. Indeed, a universally applicable solution remains elusive due to the inherent limitations of most fiber candidates in various regimes. Instead, it is imperative to conduct comprehensive studies on fiber characteristics, such as transmission loss, coupling coefficient with other devices, group velocity dispersions, and structural flexibility, to determine optimum solutions for given scenarios.

Short-range fiber links can be used for signal delivery between discrete terahertz devices, where one tends to focus on the impact of the coupling coefficient. A ubiquitous scenario is the transition between chips and three-dimensional rectangular waveguides, which is of necessity for the integration of various terahertz planar devices into a packaged circuit. Wire-bonding probe,[184] shaped as a freely suspended metal wire mounted on a chip substrate and inserted into a rectangular waveguide via a small feed-through opening, was reported to feature low insertion loss (less than 2 dB) and large return loss (above 10 dB) within a broadband (which is comparable with the waveguide bandwidth),[185,186] thus promising area- and cost-effective interfacing. For another much-needed short-range link application, i.e., intra/inter-chip interconnections, the hollow-core dielectric fiber of high flexibility and low transmission loss can be coupled with chips via their integrated tapered structures for stable wired links. Using broadband carrier waves at 0.3 THz band and on-off keying modulation, Nagatsuma *et al.* demonstrated error-free terahertz communication at 10 Gbps via a 1 m long polytetrafluoroethylene fiber.[187] Silica tubes with metalized inner surfaces featuring higher coupling efficiency with chips (~60% within a bandwidth of 150 GHz) were then reported to enable a 10 cm long 22 Gbps error-free link, as shown in Fig. 9(a).[188]

It is noted that such a metalized hollow-core fiber also fits for longer-range terahertz links. 128 Gbps and 352 Gbps signal deliveries at W-band (75–110 GHz) and 325 GHz over a meter-level range were demonstrated by Yu *et al.*[189,193] [see Fig. 9(b)]. In addition, despite the material absorption and chromatic dispersion of the hosting polymer, long-range terahertz links have been implemented by solid-core fibers,[194,195] especially the subwavelength ones with electric field predominated distributed in the air cladding for smaller transmission loss and dispersion.[196] Using a photonic-based terahertz transmitter with on-off keying (OOK) modulation [see Fig. 9(c)], Skorobogatiy *et al.* validated terahertz fiber links at operational frequency of around 140 GHz using porous fiber, rod-in-air fiber, and suspended-core fiber in polypropene sequentially.[38,123,124,197] A critical conclusion drawn from the experimental results is as follows: Meters-long rod-in-air fibers of different diameters supported error-free signal delivery with data rates of up to 4 Gbps. Instead of absorption loss, modal dispersion became the dominating limitation factor for higher data rates when reducing the fiber diameter. Such fiber-based links theoretically offer a superior power budget for short-range data transmission compared to the conventional free-space one[38] [see Fig. 9(c)]. Featuring strong modal confinement, a 0.22 m long graded-index porous fiber exhibited minimal variation in bit error rate for 6 Gbps data transmission when subjected to an increase in the bending angle, indicating its potential applications in compact environments.[197] Despite higher experimental transmission loss compared to the ideal structure, suspended-core fibers with a challenging-to-reproduce micro-sized core structure supported meters-long links with a moderate bit error rate.[123] A rectangle-shaped core fiber enabled signal delivery in modes of orthogonal linear polarization with low crosstalk.[124]

It should be noted that OOK is one of the simplest version of amplitude shift keying (ASK), where the presence and absence of carrier waves correspond to input signals of "1" and "0," respectively. In most terahertz wired links using such modulation format, the insertion loss, operation bandwidth, and modal dispersion of employed terahertz fibers have a great impact on their performance. The attenuation of transmitted terahertz signal is predominantly governed by the transmission loss of stand-alone fiber and its coupling coefficient with other devices. With registered power falling below the decision threshold of terahertz receivers for clear channel, BER of terahertz signals deteriorates due to the low signal-to-noise ratio (SNR), especially for high data rate transmission. In addition, according to the Shannon–Hartley theorem, the fiber operational bandwidth B along with the SNR imposes limits on the channel capacity C, which denotes the theoretical upper bound of data rates by[198]

$$C = B\log_2(1 + SNR). \tag{10}$$

Moreover, fiber modal dispersion induces temporal spreading of transmitted pulses, thus resulting in somewhat overlaps between successive pulses. When considering the fiber GVD exclusively, a maximal allowable bit rate can be approximated as $1/4\sqrt{GVD * L}$, where L refers to the fiber length, and the factor of 4 is determined by the requirement that ~95% of the power of the broadened pulse form

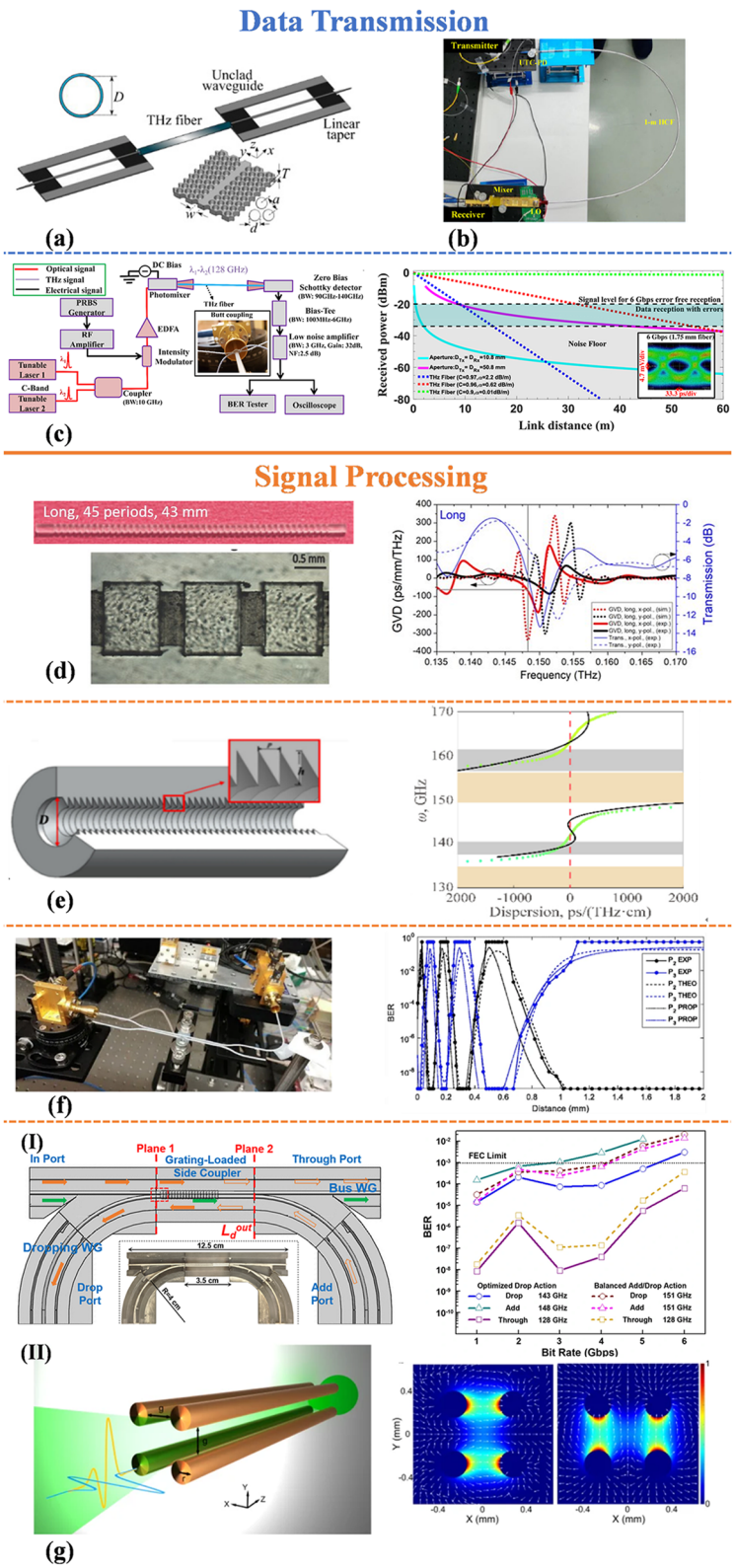

FIG. 9. Demonstrations of terahertz waveguide components for terahertz communications. (a) Metallized silica tube for inter-chip interconnection, reproduced with permission from[188] Koala *et al.*, Opt. Express **31**, 7351–7362 (2023). Copyright 2023 The Optical Society. (b) Metallized hollow-core fiber for a long-range link, reproduced with permission from[189] Ding *et al.*, Digital Commun. Networks **9**, 717–722 (2023). Copyright 2023 Author(s), licensed under a Creative Commons Attribution 4.0 License. (c) Photonic-based terahertz wired communication system based on rod-in-air dielectric fiber, together with its comparison with the wireless communication in power budget, reproduced with permission from[38] Nallappan *et al.*, Photonics Res. **8**, 1757–1775 (2020). Copyright 2020 Author(s), licensed under a Creative Commons Attribution 4.0 License. (d) Signal filter built on terahertz subwavelength rod-in-air dielectric fiber and simulated GVDs (blue curves), transmission spectra (red curves) under x (solid curves) and y (dashed curves) polarizations, reproduced with permission from[31] Ali Khan *et al.*, Opt. Express **30**, 8794–8803 (2022). Copyright 2022 The Optical Society. (e) Dispersion compensator built on terahertz hollow-core fiber having metallized periodical corrugations, as well as its dispersion relationship arising from the experimental measurement (solid black line) and the theoretical calculation (colored dots), reproduced with permission from[181] Ma *et al.*, Opt. Express **25**, 11009–11026 (2017). Copyright 2017 The Optical Society. (f) Coupler built on terahertz rod-in-air dielectric fiber and the output-ports intensity of main line (P2) and coupling line (P3) at different distances, reproduced with permission from[190] Ma *et al.*, J. Infrared, Millimeter, Terahertz Waves **38**, 1316–1320 (2017). Copyright 2017 Springer Nature. (g) Channel multiplexers built on two-wire terahertz plasmonic fibers with the measured BER vs bit rate of the THz carrier wave propagating. (I) Add-drop multiplexer for frequency-division multiplexing with the measured BER vs bit rate of the THz carrier wave propagating; reproduced with permission from[191] Cao *et al.*, Nat. Commun. **13**, 4090 (2022). Copyright 2022 Author(s), licensed under a Creative Commons Attribution 4.0 License. (II) Four-wire arrangement for polarization division multiplexing along with its simulated electric field distributions of TEM_x and TEM_y modes evaluated at 0.5 THz, reproduced with permission from[192] Dong *et al.*, Nat. Commun. **13**, 741 (2022). Copyright 2022 Author(s), licensed under a Creative Commons Attribution 4.0 License.

remains within the time slot for logical "1". As for other advanced modulation formats (for example, the quadrature phase shift keying), additional considerations related to terahertz fibers should be addressed, which extends beyond the scope of this tutorial.

We should note that the emerging terahertz fiber links are not intended to replace terahertz wireless communications for data transmission, even though by leveraging the advantages of terahertz fibers in strong electric field confinement and immunity to external disturbances, one can compensate the intrinsic deficiencies of terahertz wireless communications in the susceptibility to atmospheric weather conditions, eavesdropping, and crosstalk in dense networks. Therefore, terahertz fiber links can operate as a contingency system for the wireless one while unlocking prospects in secure high-speed communications. In 2018, a fully packaged 130 GHz transmitter achieved data rates of tens of Gbps over a one m dielectric fiber link.[195] After that, experimental results demonstrated that terahertz hollow-core fiber has attained an unprecedented benchmark of several hundred Gbps for wired terahertz link.[199] In addition, due to its flexibility in modal field design and bendable nature, a terahertz fiber enables the propagation of the terahertz signal over complex geometrical paths without trivial alignments while offering stable coupling to transceivers. It greatly simplifies the construction of non-line-of-sight and intra/inter-chip links for both static and dynamic operations. More importantly, in addition to facilitating information transportation, terahertz fiber devices can serve as multifunctional tools for efficient manipulation of terahertz signals within the terahertz networks, thereby enhancing the overall performance of terahertz communications through exploiting the degrees of freedom of terahertz optics.

Despite the extensive demand for signal processing in the spectral domain, such as signal filtering and dispersion management in communication systems, fiber Bragg gratings (FBGs)—a widely used solution in the infrared range (i.e., the well-known optic-communication regime)—are still in their nascent stage with a few demonstrators based on fibers of simple structure in the terahertz range. Using the standard quarter-wave condition, the Bragg wavelength (λ_{Bragg}) can be expressed as follows,[30] where Λ is the period and n_{eff} is the effective refractive index of the FBG:

$$\lambda_{Bragg} \approx 2\Lambda n_{eff}. \tag{11}$$

Consequently, the FBGs with stopband at the desired spectral position (i.e., λ_{Bragg}) can be designed for both bands. Different from the established infrared solutions using photosensitive hosting material and supporting RI tuning via UV radiation, periodical variations in fiber effective refractive index were rather achieved by periodically varying the fiber cross section in the terahertz band. Theoretically, the high uniformity of the grating structure and its intensified modal field confinement ensure high reflectance and low transmittance within a wide bandwidth, while the primary challenge resides in the experimental implementation of stand-alone structures having acceptable precision using conventional methods.

Superimposing periodical features on terahertz subwavelength rod-in-air fibers has been readily achievable via various post-processing processes {for example, circularly asymmetric inscriptions using excimer laser ablation[200] and rectangular-shaped geometrical birefringence ones using high-precision milling[26] [see Fig. 9(d)]}, resulting in transmission dips of high extinction ratio at the desired spectral position. In addition, signal filtering functionality has also been realized by two-wire waveguides with the assistance of wire-integrated and additional planar grating structures, respectively. For the former design, compared to the 3D printed one consisting of a corrugated wire,[191] the Bragg grating with a notch sequence processed by metal dicing using a diamond blade features a higher Q-factor.[192] Band isolating was also demonstrated by engineering two multiscale groove structures of distinct topological invariants, resulting in topological interface states within two-wire waveguides.[201] While for the later solution, a paper sheet containing a laser-cut slit array or hot-stamped metalized pattern was inserted into the air gap between wires,[32,202] thus imposing effective periodic perturbation to the two-wire waveguide. Such a design confronts a lower threshold entering into production but comes at the expense of reduced reflectance within its grating stopband, thereby limiting its applications.

Dispersion compensators, which are capable of temporally suppressing terahertz pulses, are indispensable for ultra-high-bit-rates long-range terahertz wireless communications (for example, satellite-to-ground links), as well as most terahertz wired links due to the noteworthy signal degradation along the transmission medium. The frequency-dependent effective refractive index of terahertz fibers leads to pulse broadening, as different frequencies propagate at varying velocities, resulting in the distortion of terahertz signals. In the case of wired links constructed with terahertz fibers exhibiting normal dispersion, where lower frequencies reach the output end first, the incorporation of dispersion compensators—short-length fiber devices featuring negative GVD—can facilitate high maximal bit rate data transmission. To meet this demand, Ma *et al.* demonstrated a 3D-printed hollow-core fiber having periodical corrugations on its metalized inner surface[181] [see Fig. 9(e)]. Due to avoiding crossing between supported fundamental and high order modes, waveguide Bragg gratings in such a design, which are highly compatible with terahertz hollow-core fiber links, were found to exhibit negative GVD on the level of hundreds ps/(THzcm) within a several-GHz bandwidth for D-band operation (110–170 GHz). A rod-in-air COC fiber-based birefringent grating was then demonstrated by Ali Khan *et al.*[31] Compared to the hollow-core fiber solution, it features larger negative GVD with higher transmission loss at the target spectral position, i.e., at the edge of the grating stopband.

Terahertz fiber coupler can serve as a splitter and combiner to manipulate terahertz power in the spatial domain, enabling allocating terahertz signals into different ports in terahertz communication systems. Y couplers, which are shaped as two coalescing terahertz fibers, can equally split broadband terahertz radiation into two arms via the junction with insertion loss mainly attributed to the transmission loss of bare fibers. Directional couplers, in the form of two adjacent terahertz fibers, can distribute input terahertz signals into two arms with a length-dependent power ratio. Experimental implementations of these two devices based on solid-core polymer fiber and two-wire waveguides have been reported in Refs. 32, 191, 190, and 203 [see Fig. 9(f) for a demonstration of solid-core polymer fiber-based coupler]. In addition, a 1 × 3 multimode interference splitter was implemented on terahertz solid-core fiber, where constructive interference results in three maxima at the end of the rectangle-shaped coupling section for output.[203]

Multiplexing, where multiple signals are consolidated into a single composite one and transmitted over a shared link, opens up new exciting perspectives for multiplying the data-through the capacity of terahertz communication network. However, compared to the silica-fiber-based infrared ones, terahertz multiplexing technologies are still in the early development with only a few preliminary demonstrators based on terahertz meta-surface,[204,205] 2D/3D waveguide,[206,207] and fibers. In terms of terahertz fiber-based solutions, considering the limited capacity of a single discrete element, one usually has to resort to integrated circuits to realize the desired complicated functions. Cao *et al.* reported a four-port add–drop multiplexer based on two-wire fiber for frequency division multiplexing.[191] Grating-loaded directional coupler, the key element of this circuit, allows spatially separating add and drop channels for terahertz wavelengths that fall within the grating stopband while letting the other wavelengths within the coupler bandwidth pass through. (De)multiplexing of terahertz signals of different carrier frequencies with bit rates of up to 6 Gbps was experimentally demonstrated by this circuit [see Fig. 9(g)]. In Ref. 192, Dong *et al.* conducted terahertz signal polarization division multiplexing using a terahertz fiber bundle in a four-metal-wires geometry. Taking advantage of the intrinsic characteristic of the two-wire fiber, this design allows independent propagation of two THz pulses multiplexed along two orthogonal polarization axes [see Fig. 9(g)]. Another polarization division multiplexing demonstrator is based on a rectangle-shaped solid-core COC fiber, where two directional couplers enable spatial separation and combination of x- and y-polarized terahertz signals, respectively.[208]

It is noted that different from the matured fiber-optic communications, where commercial silica fiber devices have been used for both data transmission and signal processing, terahertz fiber-assisted communications are still in the nascent stage of development. The deficiencies in specific optical properties, including the transmission loss, bending loss, and group velocity dispersion along with limitations in structural flexibility pose challenges for the aforementioned terahertz fibers to serve as ubiquitous terahertz communication platforms. Considering the lack of universal design standards and manufacturing routes, the majority of reported terahertz fiber devices are passive ones, where signal processing functionalities with fixed performance are achieved by pre-designing the fiber macrostructure and leveraging its characteristics. As for complex functionalities such as terahertz generation, signal modulation, and optical switching, which are not achievable with standalone fiber devices, integration with materials having tunable properties and other active devices is necessary; however, there have been few reported cases.[209,210] Furthermore, while in most studies, some of the desired communication functionalities have been demonstrated by discrete terahertz fiber devices, there remains a notable dearth of consideration given to the device compatibility and system integration for practical applications.

In summary, terahertz fiber-assisted communications, particularly operating at higher terahertz frequencies, is attractive as it can enable large bandwidth data channels (several hundreds of GHz) even without complex multiplexing schemes. As any fiber optics does, terahertz fibers offer flexible delivery of physically isolated data without the complexities of inter-channel crosstalk typical for free space terahertz communications. Furthermore, forgoing complex hardware for polarization, wavelength, and other multiplexing formats (which are unavoidable in microwaves due to limited bandwidth) while retaining high bandwidths is appealing for commercial applications of terahertz technology due to cost savings. Another advantage of the terahertz spectral range is that it can be accessed using the same technique as microwaves with carrier frequency close to 1 THz reported in the literature. Therefore, all the standard machinery of RF data encoding, modulation, and demodulation can be used in the terahertz and microwave ranges without conceptual modification. This is in stark contrast to systems that use optical transceivers to carry the RF data over optical fiber, which adds major costs per channel. Despite all the potential advantages, developing terahertz fiber for high-bandwidth communications is challenging. First, the high material loss in the terahertz range (especially at higher frequencies) limits the use of single-mode fibers to only several tens of centimeters to a meter. While some multimode fibers (for instance, the hollow-core ones) can offer a longer range, they suffer from inter-modal scattering on imperfections and potential dispersion and losses. Furthermore, for long-range (generally above 10 m), high-bandwidth terahertz wired communications, fiber dispersion management becomes critical as data bandwidth might present a significant percentage of the carrier frequency. Finally, to be practical, terahertz fibers should allow mass production rates comparable with those of optical fibers, which is still a largely unresolved problem.

B. Sensing and spectroscopy

Due to the presence of certain macromolecular fingerprints, transparency of dielectrics that are opaque in the visible and near-infrared range, as well as low photon energy of the non-ionizing radiation, the terahertz band offers new possibilities for spectroscopy and sensing. On the one hand, by tracking the spectral position of absorption lines associated with intramolecular and intermolecular vibrations, in conjunction with analyzing the transmitted amplitude, one can effectively identify analytes and determine their concentrations. On the other hand, non-destructive detection and monitoring of analyte physical (for example, organic solvent viscoelasticity) and structural (for instance, the dielectric film thickness) properties have been achievable by comparing broadband amplitude and phase spectra. Terahertz spectroscopy and sensing have generally reached technology readiness level with numerous laboratory demonstrations and some industrial applications. Notably, apart from the conventional implementations via the interaction between free-space terahertz wave and target analytes in straightforward manners, some studies revealed that the incorporation of terahertz fiber devices endowed terahertz spectroscopy and sensing with superior performance and novel applications. In this section, we categorized these implementations according to the functionality of terahertz fiber devices.

Terahertz spectroscopy, which relies on the intrinsic molecular properties of the analyte itself, has been realized with the assistance of terahertz fibers, especially the one supporting broad-bandwidth operation. In Ref. 211, Matsuura *et al.* demonstrated the remote detection of theophylline using a TDS setup. The recorded terahertz pulse, which transmitted through hollow-core fiber and then reflected back by a mirror behind an analyte with 1 mm thickness, featured an absorption peak at the spectral position corresponding to the analyte characteristic frequency. Furthermore, hollow-core

fiber itself was also reported to serve as a low-volume and high-path cell for terahertz gas spectroscopy. Gaseous analytes, such as water vapor and ammonia sealed inside fibers were identified by locating the spectral position with high transmission loss on the normalized spectra.[212,213] In addition to hollow-core fiber, Walther *et al.* proposed a metal-wire-based terahertz spectrometer with open geometry in 2005 and detected lactose powder of a minimal amount dispersed on top of wire[214] [see Fig. 10(a)]. Overall, it can be said that in comparison with the conventional terahertz free-space spectroscopy, terahertz fiber-based one features a distinct advantage of improved efficiency of the interaction between terahertz radiation and target analytes, thus rendering it suitable for the investigation of weakly absorbing materials in small quantities.

Terahertz fiber-based sensing, where analyte detection depends on tracking variations in optical characteristics of the guided wave, is theoretically available through a variety of detection methods for nearly arbitrary combination of reported terahertz fibers and analytes. Nevertheless, considering the technical challenges associated with the realization of controlled and observable light/fiber interaction using accessible terahertz fiber manufacturing and characterization methods, only a few experimental implementations have emerged. One of the simplest implementations is by leveraging the evanescent wave of the terahertz subwavelength fiber. The presence of analytes in the solid phase (such as tryptophan powder[217] and *E. coli* bacteria[218] for biological applications) contributed to the effective refractive index of fiber cladding, thus leading to variations in the guided wave properties (for example, the dispersion relation[217] and transmission amplitude[218]) compared to that of bare fiber. Furthermore, the incorporation of amorphous glucose molecules into Ag nanoparticle clusters on the inner metallized surface of a terahertz hollow-core fiber leads to increased absorption and decreased reflection of terahertz-guided waves. The glucose resulting from volatilized solvents sealed within fibers of varying concentrations can be detected by analyzing its transmission amplitude.[219] In another scheme, gaseous analytes in an external chamber or inside a fiber can be remotely probed by analyzing the terahertz hollow-core fiber-guided wave, with experimental setups resembling that of terahertz fiber spectroscopy studies.[211,212] Real-time tracing of dynamic chemical reaction between HCl and NH_3 vapor outside fiber, quantitative analysis of synthesized NH_4Cl aerosols with a detection limit of 165 nmol/mm^2, as well as product distribution mapping, were demonstrated by monitoring the reflected terahertz power at 0.4 THz in Ref. 220. By monitoring two reflectivity peaks around 0.34 THz, which corresponds to high-order core-guided modes of terahertz fiber, Lu *et al.* recognized the category and density of volatile organic compounds vapors diffused into fiber core[215] [see Fig. 10(b)].

Resonance, which is inherent in terahertz fibers or intrigued by additional features, opens up another avenue for terahertz fiber-based sensing. On the one hand, in terahertz Bragg fibers, analytes (for instance, powder deposited onto core surfaces[65] and liquid flowing through channel integrated into cladding[64]) supported defect state that can hybridize with the core-guided mode. The anticrossing resonant phenomenon resulted in narrow dips and sharp changes in the measured amplitude and phase spectra, respectively, whose spectral position strongly depended on analyte properties. Powder thickness detection and real-time liquid RI monitoring with sensitivities of 0.1 GHz/μm and ~110 GHz/RIU were experimentally demonstrated by terahertz Bragg fibers for operation around 200 GHz, respectively[64,65] [see Fig. 10(c) for the demonstration of THz fluidic sensing]. Furthermore, an implementation using hollow-core sapphire PC fibers addressed a remaining challenge exposed by the lack of materials and components capable of operating under extreme conditions for terahertz sensing in harsh environments such as high temperatures and pressures.[48] The interference pattern between the two core-guided modes at the fiber output end exhibited significantly different temperature-dependent shifts when a $NaNO_2$ film was present in the fiber core, compared to a bare fiber.

On the other hand, terahertz fiber-based surface plasmon resonance (SPR) sensing, which relies on phase matching between the core-guided and surface plasmon modes, has been proposed by depositing ferroelectric polyvinylidene fluoride with a layer-thickness of tens of micrometers surrounding porous fibers[221] and metal wires.[222] Theoretically speaking, such sensor designs allow monitoring the RI change in the ambient analytes in both amplitude- and spectral-based detection methods with sensitivities of tens RIU-1 and hundreds of mm/RIU, respectively. In addition, terahertz FBGs, which are achievable by imposing periodical features on top of terahertz fibers, provide a versatile platform for various applications, including resonant sensing. Similar to Ref. 218, the paper sheets placed in direct contact with a terahertz rod-in-air FBG had an impact on its modal effective refractive index. A linear dependence of the spectral position of transmission dip in the vicinity of 375 GHz on the paper thickness enabled paper quality monitoring with a sensitivity of 0.067 GHz/mm[216] [see Fig. 10(d)]. In Ref. 223, a sequence of subwavelength grooves that were etched on the outer surface of hollow-core fiber resulted in a modulation effect on the resonance of guided terahertz wave. It also served as containers for efficiently interrogating the filled liquid analyte by evanescent terahertz field. A sensitivity of 50 GHz/μl with precision larger than 0.125 μl was demonstrated by such a microfluidic sensor. Gas sensing was experimentally implemented by a terahertz two-wire phase-shifted FBG in a modular microencapsulated design. Glycerol vapor flowing through the sealed cavity was detected in real-time by tracking the transmission peak within the grating stopband.[224]

In summary, terahertz fibers in various forms have provided a highly controllable platform for efficient interrogation of analytes using guided terahertz waves, enabling resonant/non-resonant sensing that is challenging to realize with free-space terahertz optics. However, compared to planar structures such as terahertz metamaterials and on-chip waveguides, terahertz fibers usually exhibit relatively lower sensitivity and resolution. Furthermore, it is essential to eliminate the influence of other factors (for instance, analyte quantity) and ensure that the sensors' response is solely attributed to the expected variation in analyte for practical applications of terahertz fiber-based sensing.

C. Imaging

Imaging at the terahertz band possesses intriguing features of non-destructiveness and perspective, which could be applied for biomedical engineering and antiterrorism security.[225] In contrast to the microwave band, an appealing scenario assisted by terahertz imaging is that, higher-resolution images of the surrounding environment are particularly useful in multi-user communications such as vehicular and drone networks.[226] To this end, terahertz

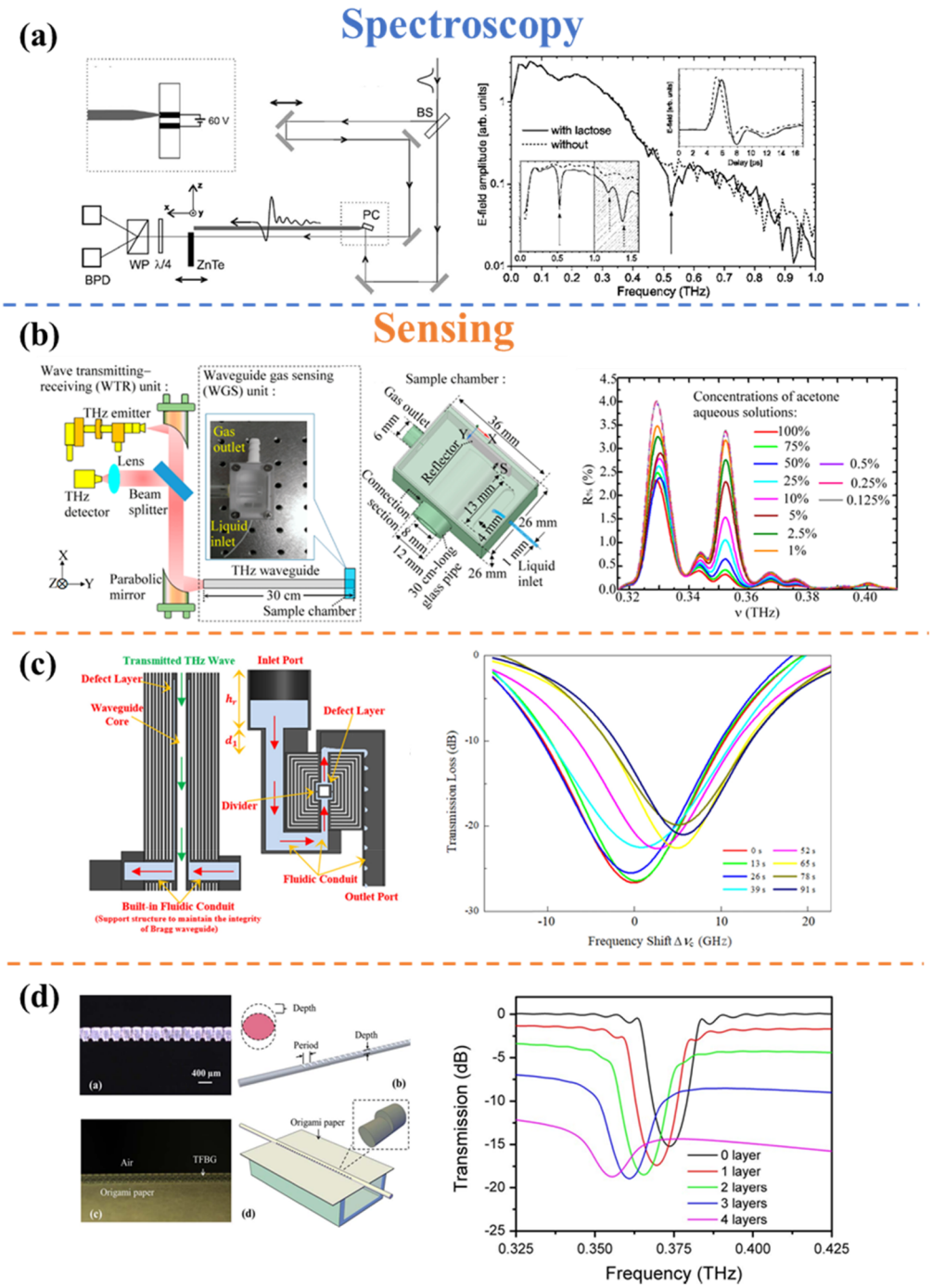

FIG. 10. Demonstrations of terahertz fiber components for terahertz spectroscopy and sensing. (a) Spectroscopy using evanescent wave supported by a terahertz metallic plasmonic fiber, and the spectra of THz pulses propagated along the fiber with (solid line) and without (dashed line) lactose, reproduced with permission from[214] Walther *et al.*, Appl. Phys. Lett. **87**, 261107 (2005). Copyright 2005 AIP Publishing LLC. (b) Remote gas sensing by tracking the amplitude spectra of a terahertz hollow-core fiber, along with reflectance spectra for different acetone concentrations in aqueous solutions, reproduced with permission from[215] Lu *et al.*, Sensors **20**, 6268 (2020). Copyright 2020 Author(s), licensed under a Creative Commons Attribution 4.0 License. (c) Dynamic RI detection of fluidic analytes by probing the anti-crossing resonant phenomenon of a terahertz Bragg fiber, together with fiber normalized transmission spectra when replacing analytes of different refractive indices in the sensing layer, reproduced with permission from[64] Cao *et al.*, Opt. Express **27**, 27663–27681 (2019). Copyright 2019 The Optical Society. (d) Paper quality monitoring enabled by terahertz dielectric FBG, as well as FBG transmission spectra for varying numbers of paper layers in direct contact, reproduced with permission from[216] Yan *et al.*, Opt. Lett. **38**, 2200–2202 (2013). Copyright 2013 The Optical Society of America.

fiber-based imaging systems are much more preferred in compact, restricted space than the bulky free-space systems.[227] In this section, several demonstrations of terahertz imaging using novel terahertz fibers will be presented.

In 2014, the flexible negative-curvature fiber fabricated using the stack-and-drawn method was presented in the context of hyperspectral imaging by scanning the end face of the fiber probe, as shown in Fig. 11(a).[82] The three transmission windows were used in a false-color image to visualize the terahertz spectral information, while detailed spectra of each pixel of the image allowed the identification of the cuvette filled with α-lactose and 4-aminobenzoic acid through their spectral fingerprints. Conventional terahertz confocal imaging generally employs conventional lenses, the resolution of which is limited by the Abbe diffraction limit. To improve the resolution performance below half of the wavelength, terahertz metallic-coated confocal fibers are proposed to replace the lenses in robust imaging systems. Two 3D-printed confocal fibers with aluminum films covered inside the inner fiber wall were successfully achieved in 2020. At 0.1 THz, high-quality images with a minimum resolution of 1.41 mm (less than 1/2 of the wavelength) were obtained by placing the imaging targets at the focus position between two fibers and performing two-dimensional scanning.[228] After that, the metallic-coated fibers realized using a wet chemical method were adopted in terahertz confocal imaging systems, achieving an enhancement of resolution up to 1.12 mm at 0.1 THz.[53] Experimental images of the USAF 1951 resolution board and a blade are shown in Fig. 11(b). Remarkably, the imaging system still maintains the same resolution when the fiber at the receiver side is bent, illustrating huge potentials of practical applications in compact, restricted space. Furthermore, terahertz fibers with special structures have also been applied for imaging systems. Flexible tapered metallic-coated fibers offer a higher energy concentration at the output, thus achieving improved penetration ability during the imaging process, as shown in Fig. 11(c).[229] Benefiting from the polarization-maintaining character, terahertz elliptical-core metallic-coated fibers supporting linearly polarized mode realize the imaging resolution of 1/3 of the wavelength at 0.1 THz.[106] Experiments also verify that the fiber is robust to bending and twisting deformation and maintains the imaging quality during flexible imaging. To further reduce the resolution, terahertz fibers based on wire-array metamaterials are experimentally demonstrated, resulting in focusing down to 1/28 of the wavelength with a net increase in power density.[230] In 2024, waveguide bundles based on low-loss hollow-core fibers have been proposed for terahertz imaging under a cryogenic environment, the spatial resolution of which is up to 400 μm, as presented in Fig. 11(d).[231] Moreover, metal-ring metamaterial structures can be placed inside the metallic hollow fibers to realize low-loss transmissions and the 1/3-wavelength imaging.[232]

In conclusion, the involvement of terahertz fibers in terahertz imaging is aimed at capturing terahertz radiation from distant targets and achieving beam focusing beyond the diffraction limit. Most relevant studies focus on improving key performance indicators of terahertz fibers, specifically reducing the transmission loss and the spot size of output radiation, thus enabling a greater distance between detectors and targets, as well as a finer spatial resolution. However, there still lies numerous practical issues; for example, to avoid power diffusing, the distance between the fiber probe and target is limited (millimeter or centimeter scale), which may hinder some application scenarios. In addition, passive imaging captures radiation emitted by objects or scattered from a uniform blackbody source without the need of an illumination source. For applications at the terahertz band, it requires terahertz detectors with extremely high sensitivity and minimal noise error. For instance, detection of human body radiation has been achieved using uncooled field-effect transistors-based one,[233] and single-photon charge-sensitive infrared phototransistors have been employed to detect near-field thermal radiation signals.[234] Furthermore, minimizing the transmission loss of terahertz signals propagating through free space or guided by terahertz fibers is crucial to ensure an adequate response of detectors to the inherently weak terahertz signals. To the best of our knowledge, there are few reports on terahertz-fiber-assisted terahertz passive imaging to date. Further research into terahertz fibers and detectors is essential to realize this technology's potential.

D. Discussions

In conclusion, it is worth noting that unlike the silica fiber devices having well-established design standards, fabrication routes, and experimental implementations for infrared operation, standardized terahertz fiber devices for specific applications are still largely absent due to the intrinsic limitation of terahertz fibers along with their challenges in accommodating functional element designs. Indeed, the majority of the reported terahertz fiber devices were developed to demonstrate their potential, rather than being driven by specific application needs. Therefore, despite there being various solutions available for different functions, only a few have advanced to practical applications. In addition to the optimization of terahertz fiber devices themselves, the seamless integration of discrete elements and their coupling with the terahertz systems is of vital importance for real-world applications (see Sec. IV B for details).

Therefore, considering the current status of relevant research, a definitive recipe for the development of terahertz fiber devices remains elusive. While there are some guidelines in terahertz fiber devices that one can follow, (1) low transmission loss and highly controllable manipulation of the guided terahertz radiation often present conflicting demands on the terahertz fiber platform geometry. In particular, a sealed structure, such as metallized tubular fibers, enables lossless data transmission while sacrificing accessibility to the mode field for signal processing. (2) Terahertz fibers in simple designs provide a superior platform for functional devices, particularly suitable for real-world applications where cost and reliability are considered. For example, although air-in-rod dielectric fibers have higher transmission and bending losses compared to porous ones, their lower threshold for implementation and deployment has facilitated more applications. 3) In addition to referencing common solutions for each frequency band (such as periodically varying the two-wire fiber cross-section for signal filter[191]), one can also resort to the unique properties of terahertz fiber for targeted functions, for example, the insertion of a planar grating structure into its exposed air gap.[32]

V. CHALLENGES AND OPPORTUNITIES

From the above-mentioned overview of developments of both terahertz fibers and corresponding devices, we would like to discuss the following two aspects that may boost the applications using terahertz fiber devices in the future.

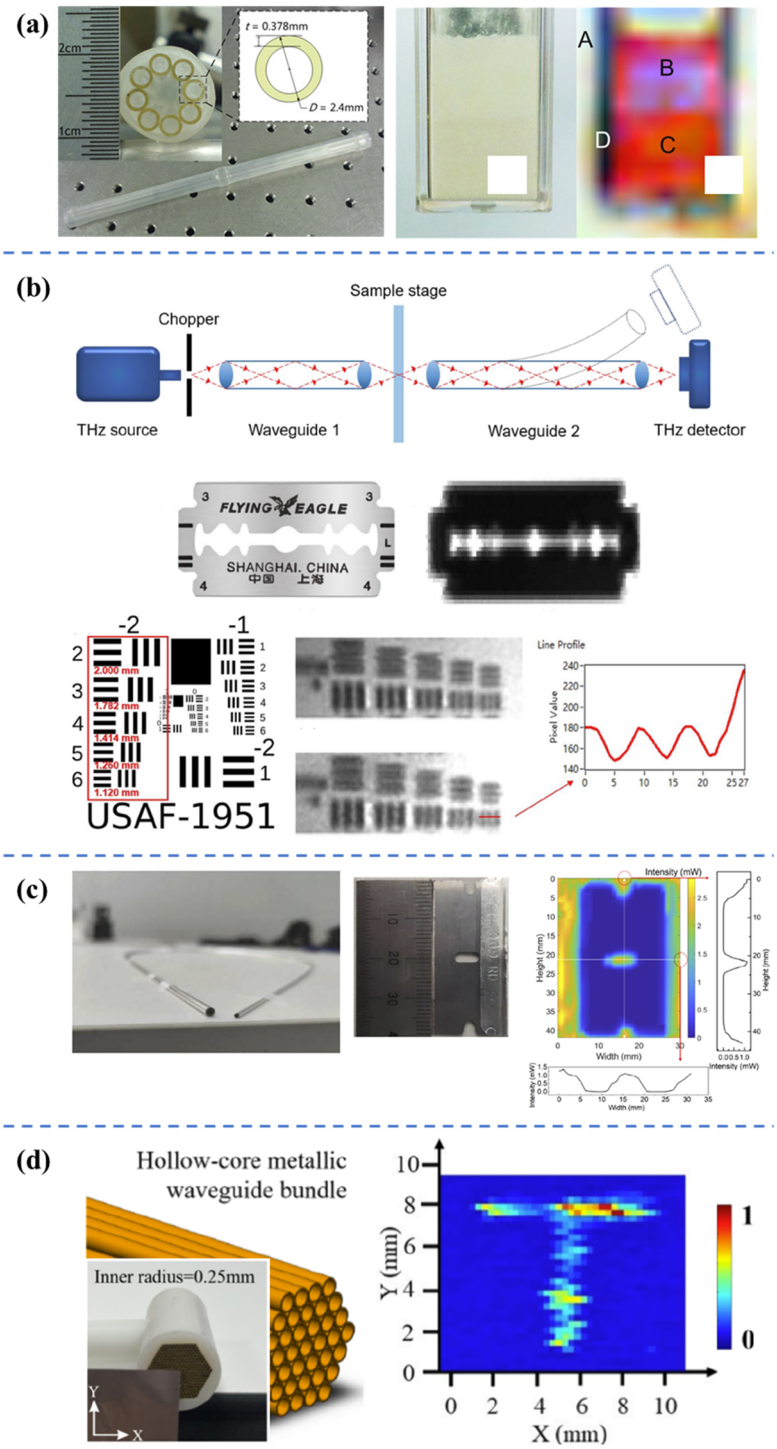

FIG. 11. Demonstrations of terahertz fiber components for terahertz imaging. (a) Flexible negative-curvature fiber for hyperspectral imaging, reproduced with permission from[82] Lu and Argyros, J. Lightwave Technol. **32**, 4019–4025 (2014). Copyright 2014 IEEE. (b) Two metallic-coated fibers for confocal imaging, reproduced with permission from[53] Liu *et al.*, IEEE Trans. Terahertz Sci. Technol. **13**, 193–199 (2023). Copyright 2023 IEEE. (c) Flexible tapered metallic-coated fibers with a higher energy concentration at the output for imaging applications, as well as terahertz imaging of blade, reproduced with permission from[229] He *et al.*, Opt. Express **29**, 8430–8440 (2021). Copyright 2021 The Optical Society. (d) A hollow-core fiber bundle for cryogenic-environment imaging and its corresponding terahertz imaging results, reproduced with permission from[231] Chen *et al.*, ACS Photonics **11**, 3068 (2024). Copyright 2024 American Chemical Society.

A. How to improve the performance of fiber devices?

Pursuing high-performance fiber devices has always remained in the field of terahertz science and technology. The foremost attribute to be improved is the propagation losses of terahertz fibers or the insertion loss of fiber devices, so as to reduce power consumption (considering the low excitation efficiency of current terahertz sources) or realize long-range transmission. In addition, low losses over a wide frequency range are in huge demand to fully utilize the broad terahertz bandwidth since fiber losses are usually frequency-dependent. Given the scarcity of materials that exhibit both low absorption and high refractive index—essential for satisfying mode guiding mechanisms—we believe innovative techniques and updates of conventional methods of terahertz fiber fabrication would be effective solutions to reduce losses at current stage. Two critical factors in this context are the smoothness of the fiber surface and the structural uniformities in both cross-sectional and longitudinal directions. A demonstrator, which confirms the significance of the above-mentioned two factors, is an infinity 3D-printed polypropylene suspended core-fiber designed for D-band operation. The post-processing annealing, aimed at surface relaxation and internal defect closure driven by polymer surface tension, resulted in a nearly 50% reduction in fiber transmission loss.[124] Currently, the alumina inner-coated hollow-core fiber, despite of its rigid and imperfect structure, has achieved a record with a minimal experimental loss of 0.025 dB/m at 160 GHz,[52] and served as an inspiring example in this field.

Furthermore, we envision that a higher-level requirement of terahertz fiber devices would be the accurate manipulation of guided waves, where the preliminary target is stable, single-mode, lossless propagation similar to the scandalized metallic WR waveguides at terahertz. In terms of hollow-core fibers, the difficulty in the pursuit of single-mode propagation lies in the trade-off between the losses and the cutoffs of high-order modes, since the oversized air-core is beneficial for decreasing losses, yet resulting in a multi-mode propagation that would excite problematic high-order modes for fiber bending or twisting. The rod-in-air dielectric fiber also suffers from a dilemma regarding the core size, which requires a compromise in the fiber structural design to balance the material absorption of the hosting material and the scattering loss due to weak modal confinement, two factors ultimately affecting its transmission loss. In addition, another imminent target revolves around terahertz signal processing with flexibility and efficiency to exploit various degrees of freedom of terahertz wave, which requires a terahertz fiber to serve as a versatile platform. Drawing inspiration from well-established infrared and microwave solutions, the terahertz fibers have to possess the capability to support highly controllable macro- and microscopic deformation, as well as incorporate deeply subwavelength-to-wavelength-sized features. The pursuit of meticulous tailoring of terahertz fiber platform design, complemented by advancements in hosting materials and fabrication routes, represents a cutting-edge focus in current research.

Improving the performance of terahertz fibers necessitates not only minimizing transmission losses but also achieving precise control over guided waves to satisfy requirement of various applications. In this context, the rapid development of artificial intelligence offers new solutions for fiber design. Through machine learning, researchers can efficiently explore innovative designs via inverse optimization, particularly in customizing fiber parameters for specific application scenarios such as communication distances, thereby significantly enhancing design efficiency and device performance. In comparison with the conventional design of devices, i.e., the sweep of multiple parameters, machine learning provides an inverse design process based on a significant volume of data, allowing researchers explore complicated, or even extraordinary, structures and meta-arrays that may have enhanced performance. Orienting to specific terahertz applications, we believe that the fiber device designs should be customized accordingly, where machine learning would be the most promising candidate for a fast, smart design. Taking terahertz fiber-based wired communication as a simple instance here, the fiber parameters need to be individualized, since the fiber loss and dispersion play dependent roles on communication performance for long- or short-range scenarios. To this end, one could design fiber parameters using machine learnings in the context of specific communication range with its optimal performance, rather than sweeping all the parameters each time for that.

B. How to apply fiber devices for real-world systems?

Since the exploration of terahertz fibers starts far later than traditional optical silica fibers, their structure has not yet been standardized, and manufacturing standards remains inconsistent. For the design and optimization process of terahertz fibers, trade-offs are frequently required between various performance metrics, where enhancing specific parameter may come at the expense of others. In addition, despite the availability of a variety of hosting materials for terahertz fibers, most of these materials have significantly higher losses compared to silica at infrared band. The aforementioned factors obstruct the advancement of standardization and technological maturity of terahertz fiber technology.

In addition to further exploration within terahertz fibers themselves, the coupling between fiber devices, which is essential for the development of compact and robust terahertz systems, also contribute to the insertion loss of terahertz signal transmission. We highlight this issue here since the scarcity of relevant research has considerably impeded the real-world applications of terahertz fiber devices. At the neighboring spectral ranges of terahertz, fusion splicing for reliable joints between silica fibers, as well as fundamentally connecting components including flanges and adaptors have been commercially available. Conversely, the absence of universal standards for the material, design, and fabrication route led to terahertz fiber devices remaining as standalone components, rather than being integrated into fiber-based circuits, within terahertz systems for complicated functionalities. In most cases, their applications require accurate alignment using complicated free-space optical devices or highly customized coupling structures, together with professional skills, even for laboratory research involving the measurement of fiber loss, and bandwidth among other fundamental attributes. On the one hand, this would lead to severe inaccuracies and unpredictably long time for the cut-back measurement (particularly using the TDS system) due to the demand of averaging data from multiple testing of fiber samples with varied lengths. On the other hand, compared to incorporating terahertz fiber devices, utilizing free-space elements to guide and manipulate terahertz radiation, despite their inevitable drawbacks in stability and tunability, is more favorable in the construction of terahertz systems at the current stage.

Considering the formidable challenge (if not impossible) of developing splicers suitable for terahertz fibers in various hosting materials and cross-sectional designs, the modular architecture of terahertz fiber devices holds greater promise for experimental realization to facilitate their practical applications. In contrast with the painstaking optical alignment of individual elements, the physical integration of devices on the same fiber platform can be obtained with ease and precision. An inspiring demonstrator is a reconfigurable plasmonic circuit built on 3D-printed micro-encapsulated two-wire fibers having connecting features at their ends. Its overall performance exhibits a high level of flexibility and stability, allowing for the addition and adjustment of target functions via plugging and replacing of modular devices,[32] thereby fulfilling the fundamental requirements for real-world applications. In addition, as the metallic WR waveguide is currently the only terahertz waveguide with a standardized design, and has been adopted for both electrical (frequency "convert-up," such as multipliers frequency extenders) and photonic (frequency "convert-down," such as photomixers) terahertz devices, there is a growing trend toward developing coupling elements that bridge various fiber devices with the WR waveguide.[22,23] With the involvements of efficient coupling elements, we foresee the standardization of terahertz fiber characterization and the seamless integration of terahertz fibers in various designs, each leveraging its unique strengths for terahertz systems with complicated functionalities.

Another challenge impeding the practical application of terahertz fibers lies in the external interference to the guided wave that propagates along complex paths. While straight-in-line terahertz fibers remain the predominant topic in academic research, curved fibers are much preferable for practical applications. On the one hand, the pliable structure, which enables easy fiber handling and compact terahertz fiber-based system, has been readily achievable by some fibers with relatively simple cross-sectional design, such as tubular, rod-in-air and suspended-core fibers. On the other hand, the desired high refractive index and low material absorption of hosting material for low scattering loss at bends, which is impossible for most polymers, has become available by polymer matrix composites. Furthermore, it is essential to reinforce terahertz fibers against mechanical and environmental stresses, such as humidity, abrasion, thermal shock, and excessive bending-induced fracture for practical applications.[235] Plastic coating, which is translated from the commercial infrared silica fiber, is theoretically suitable for terahertz dielectric fibers, especially the ones featuring strong modal confinement in its central core. In the context of terahertz bare fibers with modal fields partially distributed in the surrounding air cladding (for instance, polyethylene rod-in-air fiber), we envision that the advancement of air-like materials at the terahertz band could open up prospects of fiber packaging via a simple insertion.[236]

One of the most appealing properties of waveguides is the ability of device integration, i.e., the well-known system-on-chip and lab-on-fiber for electronics and optical fibers, respectively. Terahertz fibers have been demonstrated as exceptional platforms for integrating diverse passive devices, the applications of which vary from communications to sensing and imaging, as we have discussed in Sec. IV. Nevertheless, we summarize the following three aspects that efforts could continue to make. First, a large amount of terahertz power is distributed in the air-region to decrease losses, yet leading to relatively weak interaction between the terahertz wave and the matter. As a result, for some applications such as sensing, the response of fiber sensors remains a scope of improvement. One promising candidate is designing meta-atoms structured on terahertz fibers to enhance the interaction. Second, in contrast to the terahertz silicon planar devices, terahertz fibers are more challenging to integrate multiple functionalities due to their cylindrical shape. Nonetheless, we should note that the fibers provide a unique feature that the devices can be integrated in three-dimensional space assisted with the cutting-edge 3D printers, which is difficult for silicon microfabrication—generally integrating devices in a two-dimensional flat wafer. Third, turnabilities are expected to be included for fiber devices based on controllable materials (such as graphene and phase-change materials) and geometric deformations of flexible fibers.

VI. CONCLUSION

In this tutorial, we present an overview of terahertz fibers and fiber-based functional devices, which are promising candidates for terahertz system integration. According to the fiber structures, the guiding mechanisms and research progress of both hollow-core and solid-core fibers are comprehensively presented in Sec. III. Section IV presents the most recent achievements of fiber devices toward terahertz applications including wired communications, sensing (spectroscopy), and imaging. In Sec. V, we propose four aspects of challenges of terahertz fiber devices that prevent the proof-of-concept research from stepping into real-world applications. The tremendous opportunities include not only the innovative designs of fiber-integrated devices using new structures, materials, and artificial intelligence methods toward a performance upgrade but also practical technologies such as high-efficient coupling integrations, and standardized, convenient characterizations of terahertz fiber devices in terms of commercialization of terahertz systems in the coming future.

The fiber, as one of the most fundamental components at the physical layer for terahertz waves propagating in both short- and long-range, is no doubt inevitable for terahertz systems. Thereby, we expect that the development of flexible, low-loss, wideband terahertz fibers with practical implementations would immensely boost the advancement of terahertz science and technology, similar to the terahertz sources and detectors that have become commercially available in the 2000s. Finally, it is reasonable to envisage that, as an ultimate goal, compact and robust terahertz systems will be constructed through the integration of fascinating terahertz fibers and devices with rich functionalities.

ACKNOWLEDGMENTS

The authors thank Xing Li, Li Wang, Xiangjun Liu, Jingxin Lu, Siqi Jia, Haiyuan Ge, and Babak Yahiapour for proofreading and insightful discussions. Haisu Li acknowledges the support from the National Natural Science Foundation of China under Grant Nos. 62475011 and 62075007. Yang Cao acknowledges the support from the National Natural Science Foundation of China under Grant No. 62205100, the Natural Science Foundation of Tianjin under Grant No. 23JCQNJC01080, the Natural Science Foundation of Hebei under Grant No. F2024202034, and the Science and Technology Cooperation Special Project of Shijiazhuang under

Grant No. SJZZXA23003. Maksim Skorobogatiy acknowledges support from the Discovery grant from the Natural Sciences and Engineering Research Council of Canada. Shaghik Atakaramians acknowledges support from the Linkage Project from the Australian Research Council under Grant No. LP210200524.

AUTHOR DECLARATIONS

Conflict of Interest

The authors have no conflicts to disclose.

Author Contributions

H. L. and Y. C. contributed equally to this tutorial.

Haisu Li: Conceptualization (equal); Funding acquisition (equal); Supervision (equal); Visualization (equal); Writing – original draft (equal); Writing – review & editing (equal). **Yang Cao**: Conceptualization (equal); Funding acquisition (equal); Visualization (equal); Writing – original draft (equal); Writing – review & editing (equal). **Maksim Skorobogatiy**: Supervision (equal); Writing – original draft (supporting); Writing – review & editing (equal). **Shaghik Atakaramians**: Conceptualization (equal); Supervision (equal); Writing – original draft (supporting); Writing – review & editing (equal).

DATA AVAILABILITY

The data that support the findings of this study are available from the corresponding author upon reasonable request.

REFERENCES

[1] D. M. Mittleman, "Perspective: Terahertz science and technology," J. Appl. Phys. **122**(23), 230901 (2017) (in English).
[2] A. Kumar, M. Gupta, and R. Singh, "Topological integrated circuits for 5G and 6G," Nat. Electron. **5**(5), 261–262 (2022) (in English).
[3] A. Leitenstorfer *et al.*, "The 2023 terahertz science and technology roadmap," J. Phys. D: Appl. Phys. **56**(22), 223001 (2023) (in English).
[4] G. Xu and M. Skorobogatiy, "Wired THz communications," J. Infrared, Millimeter, Terahertz Waves **43**(9-10), 728–778 (2022).
[5] See https://www.vadiodes.com for information about commercialized terahertz metallic waveguides.
[6] S. Atakaramians, S. Afshar V, T. M. Monro, and D. Abbott, "Terahertz dielectric waveguides," Adv. Opt. Photonics **5**(2), 169–215 (2013) (in English).
[7] W. Withayachumnankul, M. Fujita, and T. Nagatsuma, "Integrated silicon photonic crystals toward terahertz communications," Adv. Opt. Mater. **6**(16), 1800401 (2018) (in English).
[8] J. Carter, H. Lees, Q. G. J. Wang, S. J. Chen, S. Atakaramians, and W. Withayachumnakul, "Terahertz properties of common microwave dielectric materials," J. Infrared, Millimeter, Terahertz Waves **44**(11-12), 873–884 (2023) (in English).
[9] D. Headland, M. Fujita, G. Carpintero, T. Nagatsuma, and W. Withayachumnankul, "Terahertz integration platforms using substrateless all-silicon microstructures," APL Photonics **8**(9), 091101 (2023).
[10] A. Kumar, M. Gupta, P. Pitchappa, N. Wang, M. Fujita, and R. Singh, "Terahertz topological photonic integrated circuits for 6G and beyond: A perspective," J. Appl. Phys. **132**(14), 140901 (2022) (in English).
[11] H. S. Li *et al.*, "Broadband single-mode hybrid photonic crystal waveguides for terahertz integration on a chip," Adv. Mater. Technol. **5**(7), 2000117 (2020) (in English).
[12] M. T. A. Khan, H. S. Li, N. N. M. Duong, A. Blanco-Redondo, and S. Atakaramians, "3D-Printed terahertz topological waveguides," Adv. Mater. Technol. **6**(7), 2100252 (2021).
[13] H. S. Li, Y. Zhang, Y. J. Liu, and S. Atakaramians, "Terahertz hybrid topological chip for 10-Gbps full-duplex communications," Electronics **12**(1), 109 (2023) (in English).
[14] M. S. Islam, C. M. B. Cordeiro, M. A. R. Franco, J. Sultana, A. L. S. Cruz, and D. Abbott, "Terahertz optical fibers [Invited]," Opt. Express **28**(11), 16089–16117 (2020) (in English).
[15] A. Markov, H. Guerboukha, and M. Skorobogatiy, "Hybrid metal wire–dielectric terahertz waveguides: Challenges and opportunities [Invited]," J. Opt. Soc. Am. B **31**(11), 2587–2600 (2014).
[16] G. F. Xu and M. Skorobogatiy, "3D printing technique and its application in the fabrication of THz fibers and waveguides," J. Appl. Phys. **133**(21), 210901 (2023) (in English).
[17] K. Tsuruda, M. Fujita, and T. Nagatsuma, "Extremely low-loss terahertz waveguide based on silicon photonic-crystal slab," Opt. Express **23**(25), 31977–31990 (2015).
[18] Y. Yang *et al.*, "Terahertz topological photonics for on-chip communication," Nat. Photonics **14**(7), 446–451 (2020).
[19] M. Gupta, A. Kumar, and R. Singh, "Electrically tunable topological notch filter for THz integrated photonics," Adv. Opt. Mater. **11**(23), 2301051 (2023).
[20] A. Kumar *et al.*, "Phototunable chip-scale topological photonics: 160 Gbps waveguide and demultiplexer for THz 6G communication," Nat. Commun. **13**(1), 5404 (2022).
[21] S. Atakaramians *et al.*, "Direct probing of evanescent field for characterization of porous terahertz fibers," Appl. Phys. Lett. **98**(12), 121104 (2011).
[22] Q. G. J. Wang, S. D. A. Shah, H. S. Li, B. Kuhlmey, and S. Atakaramians, "20 dB improvement utilizing custom-designed 3D-printed terahertz horn coupler," Opt. Express **31**(1), 65–74 (2023) (in English).
[23] R. Viratikul, B. B. Hong, P. Janpugdee, J. Oberhammer, I. D. Robertson, and N. Somjit, "220–325-GHz horn-type adapter for terahertz microstructured fiber measurements," IEEE Trans. Instrum. Meas. **73**, 8001910 (2024) (in English).
[24] A. Barh, B. P. Pal, G. P. Agrawal, R. K. Varshney, and B. M. A. Rahman, "Specialty fibers for terahertz generation and transmission: A review," IEEE J. Sel. Top. Quantum Electron. **22**(2), 365–379 (2016).
[25] B. M. A. Rahman *et al.*, "Optical fiber, nanomaterial, and THz-metasurface-mediated nano-biosensors: A review," Biosensors **12**(1), 42 (2022).
[26] H. Li *et al.*, "Terahertz polarization-maintaining subwavelength dielectric waveguides," J. Opt. **20**, 125602 (2018).
[27] H. Xiao, H. S. Li, B. L. Wu, Y. Dong, S. Y. Xiao, and S. S. Jian, "Low-loss polarization-maintaining hollow-core anti-resonant terahertz fiber," J. Opt. **21**(8), 085708 (2019) (in English).
[28] H. Xiao, H. S. Li, B. L. Wu, and S. S. Jian, "Polarization-maintaining terahertz bandgap fiber with a quasi-elliptical hollow-core," Opt Laser. Technol. **105**, 276–280 (2018) (in English).
[29] Y. J. Liu, M. T. A. Khan, S. Atakaramians, and H. S. Li, "Terahertz polarization-maintaining sampled gratings for dual-frequency filtering and dispersion compensation," Res. Phys. **39**, 105721 (2022) (in English).
[30] H. Li *et al.*, "Terahertz polarization-maintaining subwavelength filters," Opt. Express **26**(20), 25617 (2018).
[31] M. T. Ali Khan, H. Li, Y. Liu, G.-D. Peng, and S. Atakaramians, "Compact terahertz birefringent gratings for dispersion compensation," Opt. Express **30**(6), 8794–8803 (2022).
[32] Y. Cao, K. Nallappan, H. Guerboukha, G. Xu, and M. Skorobogatiy, "Additive manufacturing of highly reconfigurable plasmonic circuits for terahertz communications," Optica **7**(9), 1112–1125 (2020).
[33] Y. S. Jin, G. J. Kim, and S. G. Jeon, "Terahertz dielectric properties of polymers," J. Korean Phys. Soc. **49**(2), 513–517 (2006) (in English).
[34] S. Wietzke *et al.*, "Terahertz spectroscopy on polymers: A review of morphological studies," J. Mol. Struct. **1006**(1-3), 41–51 (2011).
[35] M. Skorobogatiy, *Nanostructured and Subwavelength Waveguides: Fundamentals and Applications* (John Wiley & Sons, 2012).
[36] X. Zhang, Y. L. Chen, R.-S. Liu, and D. P. Tsai, "Plasmonic photocatalysis," Rep. Prog. Phys. **76**(4), 046401 (2013).

[37]H. L. Bao, K. Nielsen, O. Bang, and P. U. Jepsen, "Dielectric tube waveguides with absorptive cladding for broadband, low-dispersion and low loss THz guiding," Sci. Rep. **5**, 7620 (2015) (in English).
[38]K. Nallappan, Y. Cao, G. Xu, H. Guerboukha, C. Nerguizian, and M. Skorobogatiy, "Dispersion-limited versus power-limited terahertz communication links using solid core subwavelength dielectric fibers," Photonics Res. **8**(11), 1757–1775 (2020).
[39]C. H. Lai, Y. C. Hsueh, H. W. Chen, Y. J. Huang, H. C. Chang, and C. K. Sun, "Low-index terahertz pipe waveguides," Opt. Lett. **34**(21), 3457–3459 (2009) (in English).
[40]A. Dupuis, K. Stoeffler, B. Ung, C. Dubois, and M. Skorobogatiy, "Transmission measurements of hollow-core THz Bragg fibers," J. Opt. Soc. Am. B **28**(4), 896–907 (2011) (in English).
[41]Z. R. Wu, W. R. Ng, M. E. Gehm, and H. Xin, "Terahertz electromagnetic crystal waveguide fabricated by polymer jetting rapid prototyping," Opt. Express **19**(5), 3962–3972 (2011) (in English).
[42]V. Setti, L. Vincetti, and A. Argyros, "Flexible tube lattice fibers for terahertz applications," Opt. Express **21**(3), 3388–3399 (2013) (in English).
[43]J. Anthony, R. Leonhardt, A. Argyros, and IEEE, "THz guidance in air core square lattice photonic crystal fibers," in *38th European Conference and Exhibition on Optical Communications (ECOC), Amsterdam, Netherlands, 16–20 September 2012* (IEEE, New York, 2012) WOS:000349826200067.
[44]D. W. Vogt, J. Anthony, and R. Leonhardt, "Metallic and 3D-printed dielectric helical terahertz waveguides," Opt. Express **23**(26), 33359–33369 (2015) (in English).
[45]X. L. Tang *et al.*, "Elliptical metallic hollow fiber inner-coated with non-uniform dielectric layer," Opt. Express **23**(17), 22587–22601 (2015) (in English).
[46]J. Yang *et al.*, "3D printed low-loss THz waveguide based on Kagome photonic crystal structure," Opt. Express **24**(20), 22454–22460 (2016) (in English).
[47]T. Ma, H. Guerboukha, M. Girard, A. D. Squires, R. A. Lewis, and M. Skorobogatiy, "3D printed hollow-core terahertz optical waveguides with hyperuniform disordered dielectric reflectors," Adv. Opt. Mater. **4**(12), 2085–2094 (2016) (in English).
[48]G. M. Katyba *et al.*, "Sapphire photonic crystal waveguides for terahertz sensing in aggressive environments," Adv. Opt. Mater. **6**(22), 1800573 (2018).
[49]W. Talataisong *et al.*, "Hollow-core antiresonant terahertz fiber-based TOPAS extruded from a 3D printer using a metal 3D printed nozzle," Photonics Res. **9**(8), 1513–1521 (2021) (in English).
[50]A. Stefani *et al.*, "Flexible terahertz photonic light-cage modules for in-core sensing and high temperature applications," ACS Photonics **9**(6), 2128–2141 (2022).
[51]T. T. Bai, Z. Y. Dong, and M. Y. Chen, "Cascaded terahertz hollow-core Bragg waveguide: Numerical design and experimental demonstration," Appl. Opt. **62**(16), 4381–4389 (2023) (in English).
[52]K. Thackston, J. Doane, J. Anderson, M. Chrayteh, and F. Hindle, "Correction to: Measurements of dielectric lined waveguides for low loss millimeter wave and terahertz transmission," J. Infrared, Millimeter, Terahertz Waves **44**(5-6), 489 (2023) (in English).
[53]S. Liu *et al.*, "Transmission and confocal imaging characteristics of bendable ABS/Ag-coated hollow waveguide at low THz band," IEEE Trans. Terahertz Sci. Technol. **13**(3), 193–199 (2023) (in English).
[54]J. D. Joannopoulos, S. G. Johnson, J. N. Winn, and R. D. Meade, *Photonic Crystals: Molding the Flow of Light*, 2nd ed. (Princeton University Press, 2008).
[55]P. Russell, "Photonic crystal fibers," Science **299**(5605), 358–362 (2003) (in English).
[56]F. Poletti, M. N. Petrovich, and D. J. Richardson, "Hollow-core photonic bandgap fibers: Technology and applications," Nanophotonics **2**(5-6), 315–340 (2013) (in English).
[57]C. H. Brodie, I. Spotts, and C. M. Collier, "THz Bragg structures fabricated with additive manufacturing," Appl. Opt. **62**(17), 4465–4473 (2023) (in English).
[58]R. J. Yu, B. Zhang, Y. Q. Zhang, C. Q. Wu, Z. G. Tian, and X. Z. Bai, "Proposal for ultralow loss hollow-core plastic Bragg fiber with cobweb-structured cladding for terahertz waveguiding," IEEE Photonics Technol. Lett. **19**(12), 910–912 (May-Jun 2007) (in English).
[59]M. Skorobogatiy and A. Dupuis, "Ferroelectric all-polymer hollow Bragg fibers for terahertz guidance," Appl. Phys. Lett. **90**(11), 113514 (2007) (in English).
[60]B. Ung, A. Dupuis, K. Stoeffler, C. Dubois, and M. Skorobogatiy, "High-refractive-index composite materials for terahertz waveguides: Trade-off between index contrast and absorption loss," J. Opt. Soc. Am. B **28**(4), 917–921 (2011) (in English).
[61]A. L. S. Cruz, A. Argyros, X. L. Tang, C. M. B. Cordeiro, M. A. R. Franco, and IEEE, "3D-printed terahertz Bragg fiber," in *40th International Conference on Infrared, Millimeter, and Terahertz Waves (IRMMW-THz), Chinese University of Hong Kong, Hong Kong, Peoples Republic of China, 23–28 August 2015* (IEEE, New York, 2015), WOS:000376674000544.
[62]B. Hong *et al.*, "Low-loss asymptotically single-mode THz Bragg fiber fabricated by digital light processing rapid prototyping," IEEE Trans. Terahertz Sci. Technol. **8**(1), 90–99 (2018) (in English).
[63]B. B. Hong, N. Chudpooti, P. Akkaraekthalin, N. Somjit, J. Cunningham, and I. Robertson, "Investigation of electromagnetic mode transition and filtering of an asymptotically single-mode hollow THz Bragg fibre," J. Phys. D: Appl. Phys. **51**(30), 305101 (2018) (in English).
[64]Y. Cao, K. Nallappan, H. Guerboukha, T. Gervais, and M. Skorobogatiy, "Additive manufacturing of resonant fluidic sensors based on photonic bandgap waveguides for terahertz applications," Opt. Express **27**(20), 27663–27681 (2019).
[65]J. Li, K. Nallappan, H. Guerboukha, and M. Skorobogatiy, "3D printed hollow core terahertz Bragg waveguides with defect layers for surface sensing applications," Opt. Express **25**(4), 4126–4144 (2017).
[66]J. W. Li, H. Qu, and J. C. Wang, "Photonic Bragg waveguide platform for multichannel resonant sensing applications in the THz range," Biomed. Opt. Express **11**(5), 2476–2489 (2020) (in English).
[67]L. Vincetti, "Hollow core photonic band gap fiber for THz applications," Microwave Opt. Technol. Lett. **51**(7), 1711–1714 (2009) (in English).
[68]G. M. Katyba *et al.*, "Sapphire waveguides and fibers for terahertz applications," Prog. Cryst. Growth Charact. Mater. **67**(3), 100523 (2021).
[69]G. B. Ren *et al.*, "Low-loss air-core polarization maintaining terahertz fiber," Opt. Express **16**(18), 13593–13598 (2008) (in English).
[70]N. M. Litchinitser, A. K. Abeeluck, C. Headley, and B. J. Eggleton, "Antiresonant reflecting photonic crystal optical waveguides," Opt. Lett. **27**(18), 1592–1594 (2002) (in English).
[71]C. H. Lai, Y. S. Yeh, C. A. Yeh, and Y. K. Wang, "Effective bandwidth of terahertz antiresonant reflecting pipe waveguide," Opt. Express **26**(5), 6456–6465 (2018) (in English).
[72]W. Ding, Y. Y. Wang, S. F. Gao, M. L. Wang, and P. Wang, "Recent progress in low-loss hollow-core anti-resonant fibers and their applications," IEEE J. Sel. Top. Quantum Electron. **26**(4), 4400312 (2020) (in English).
[73]E. Nguema, D. Férachou, G. Humbert, J. L. Auguste, and J. M. Blondy, "Broadband terahertz transmission within the air channel of thin-wall pipe," Opt. Lett. **36**(10), 1782–1784 (2011) (in English).
[74]C.-H. Lai *et al.*, "Modal characteristics of antiresonant reflecting pipe waveguides for terahertz waveguiding," Opt. Express **18**(1), 309–322 (2010).
[75]J. T. Lu, Y. C. Hsueh, Y. R. Huang, Y. J. Hwang, and C. K. Sun, "Bending loss of terahertz pipe waveguides," Opt. Express **18**(25), 26332–26338 (2010) (in English).
[76]J.-T. Lu *et al.*, "Terahertz pipe-waveguide-based directional couplers," Opt. Express **19**(27), 26883–26890 (2011).
[77]D. W. Vogt and R. Leonhardt, "3D-Printed broadband dielectric tube terahertz waveguide with anti-reflection structure," J. Infrared, Millimeter, Terahertz Waves **37**(11), 1086–1095 (2016) (in English).
[78]C. L. Wei, R. J. Weiblen, C. R. Menyuk, and J. Hu, "Negative curvature fibers," Adv. Opt. Photonics **9**(3), 504–561 (2017) (in English).
[79]M. F. Xiao, J. Liu, W. Zhang, J. L. Shen, and Y. D. Huang, "Self-supporting polymer pipes for low loss single-mode THz transmission," Opt. Express **21**(17), 19808–19815 (2013) (in English).
[80]M. M. Nazarov *et al.*, "Eight-capillary cladding THz waveguide with low propagation losses and dispersion," IEEE Trans. Terahertz Sci. Technol. **8**(2), 183–191 (2018) (in English).
[81]W. L. Lu, S. Q. Lou, and A. Argyros, "Investigation of flexible low-loss hollow-core fibres with tube-lattice cladding for terahertz radiation," IEEE J. Sel. Top. Quantum Electron. **22**(2), 4401607 (2016) (in English).
[82]W. L. Lu and A. Argyros, "Terahertz spectroscopy and imaging with flexible tube-lattice fiber probe," J. Lightwave Technol. **32**(23), 4019–4025 (2014) (in English).

[83]A. Stefani, J. Henry Skelton, and A. Tuniz, "Bend losses in flexible polyurethane antiresonant terahertz waveguides," Opt. Express **29**(18), 28692–28703 (2021) (in English).
[84]A. Stefani, S. C. Fleming, and B. T. Kuhlmey, "Terahertz orbital angular momentum modes with flexible twisted hollow core antiresonant fiber," APL Photonics **3**(5), 051708 (2018) (in English).
[85]S. Yang, X. Z. Sheng, G. Z. Zhao, and S. Li, "Simple birefringent Terahertz fiber based on elliptical hollow core," Opt. Fiber Technol. **53**, 102064 (2019).
[86]S. Yang, X. Z. Sheng, G. Z. Zhao, Y. Wang, and Y. Yu, "Novel pentagram THz hollow core anti-resonant fiber using a 3D printer," J. Infrared, Millimeter, Terahertz Waves **40**(7), 720–730 (2019) (in English).
[87]S. Yang, X. Z. Sheng, G. Z. Zhao, S. Q. Lou, and J. Y. Guo, "3D printed effective single-mode terahertz antiresonant hollow core fiber," IEEE Access **9**, 29599–29608 (2021) (in English).
[88]L. Xue *et al.*, "Single-mode hollow-core anti-resonant waveguides for low-loss THz wave propagation," J. Infrared, Millimeter, Terahertz Waves **44**(9-10), 673–692 (2023) (in English).
[89]L. Xue *et al.*, "High-birefringence low-loss hollow-core THz waveguide embedded parallel slab cladding," IEEE Trans. Terahertz Sci. Technol. **12**(5), 471–480 (2022) (in English).
[90]L. D. van Putten, J. Gorecki, E. Numkam Fokoua, V. Apostolopoulos, and F. Poletti, "3D-printed polymer antiresonant waveguides for short-reach terahertz applications," Appl. Opt. **57**(14), 3953–3958 (2018) (in English).
[91]J. Sultana *et al.*, "Hollow core inhibited coupled antiresonant terahertz fiber: A numerical and experimental study," IEEE Trans. Terahertz Sci. Technol. **11**(3), 245–260 (2021) (in English).
[92]J. Anthony, R. Leonhardt, S. G. Leon-Saval, and A. Argyros, "THz propagation in kagome hollow-core microstructured fibers," Opt. Express **19**(19), 18470–18478 (2011) (in English).
[93]S. Li *et al.*, "A 0.1 THz low-loss 3D printed hollow waveguide," Optik **176**, 611–616 (2019) (in English).
[94]H. S. Li *et al.*, "Guiding terahertz orbital angular momentum beams in multimode Kagome hollow-core fibers," Opt. Lett. **42**(2), 179–182 (2017) (in English).
[95]N. J. Cronin, Microwave and Optical Waveguides, 1995.
[96]R. W. McGowan, G. Gallot, and D. Grischkowsky, "Propagation of ultrawideband short pulses of terahertz radiation through submillimeter-diameter circular waveguides," Opt. Lett. **24**(20), 1431–1433 (1999) (in English).
[97]G. Gallot, S. P. Jamison, R. W. McGowan, and D. Grischkowsky, "Terahertz waveguides," J. Opt. Soc. Am. B **17**(5), 851–863 (2000).
[98]Y. Abe, Y. W. Shi, Y. Matsuura, and M. Miyagi, "Flexible small-bore hollow fibers with an inner polymer coating," Opt. Lett. **25**(3), 150–152 (2000) (in English).
[99]J. A. Harrington, R. George, P. Pedersen, and E. Mueller, "Hollow polycarbonate waveguides with inner Cu coatings for delivery of terahertz radiation," Opt. Express **12**(21), 5263–5268 (2004) (in English).
[100]M. Navarro-Cía, J. E. Melzer, J. A. Harrington, and O. Mitrofanov, "Silver-coated Teflon tubes for waveguiding at 1-2 THz," J. Infrared, Millimeter, Terahertz Waves **36**(6), 542–555 (2015) (in English).
[101]M. S. Vitiello *et al.*, "Guiding a terahertz quantum cascade laser into a flexible silver-coated waveguide," J. Appl. Phys. **110**(6), 063112 (2011) (in English).
[102]R. Wallis *et al.*, "Investigation of hollow cylindrical metal terahertz waveguides suitable for cryogenic environments," Opt. Express **24**(26), 30002–30014 (2016) (in English).
[103]S. Liu *et al.*, "A robust PEEK/silver-coated hollow waveguide for terahertz bendable transmission in hot and cold environments," Res. Phys. **35**, 105395 (2022) (in English).
[104]X. L. Tang *et al.*, "Elliptical hollow fiber with inner silver coating for linearly polarized terahertz transmission," IEEE Photonics Technol. Lett. **25**(4), 331–334 (2013) (in English).
[105]M. H. He *et al.*, "Design, fabrication, and characterization of a single-polarization single-mode flexible hollow waveguide for low loss millimeter wave propagation," Opt. Express **30**(6), 10178–10186 (2022) (in English).
[106]M. H. He *et al.*, "Low-loss flexible polarization-maintaining hollow waveguide for linearly polarized 100 GHz radiation transmission and subwavelength imaging," J. Lightwave Technol. **40**(20), 6712–6718 (2022) (in English).
[107]M. Mineo and C. Paoloni, "Improved corrugation cross-sectional shape in terahertz double corrugated waveguide," IEEE Trans. Electron Devices **59**(11), 3116–3119 (2012).
[108]J. F. Zeng, M. H. He, X. Zhang, X. S. Zhu, and Y. W. Shi, "Simulation methods and transmission characteristics of dielectric-coated metallic waveguides from mid-infrared to millimeter waves," Appl. Phys. B **127**(7), 99 (2021) (in English).
[109]B. Bowden, J. A. Harrington, O. Mitrofanov, and IEEE, "Silver/Polystyrene coated hollow glass waveguides for the transmission of THz radiation," in *Conference on Lasers and Electro-Optics/Quantum Electronics and Laser Science Conference, Baltimore, MD, 06–11 May 2007* (IEEE, New York, 2007), p. 1512, WOS:000268751001197.
[110]O. Mitrofanov, R. James, F. A. Fernández, T. K. Mavrogordatos, and J. A. Harrington, "Reducing transmission losses in hollow THz waveguides," IEEE Trans. Terahertz Sci. Technol. **1**(1), 124–132 (2011) (in English).
[111]A. Aming and M. A. Rahman, "Design and characterization low-loss modes in dielectric-coated hollow-core waveguides at THz frequency," J. Lightwave Technol. **36**(13), 2716–2722 (2018) (in English).
[112]B. Bowden, J. A. Harrington, and O. Mitrofanov, "Low-loss modes in hollow metallic terahertz waveguides with dielectric coatings," Appl. Phys. Lett. **93**(18), 181104 (2008) (in English).
[113]Y. Y. Huang *et al.*, "Suitability of metallic materials for constructing metal-coated dielectric terahertz waveguides," J. Appl. Phys. **131**(10), 105106 (2022) (in English).
[114]C. M. Bledt, J. E. Melzer, and J. A. Harrington, "Fabrication and characterization of improved Ag/PS hollow-glass waveguides for THz transmission," Appl. Opt. **52**(27), 6703–6709 (2013) (in English).
[115]M. Navarro-Cía, M. S. Vitiello, C. M. Bledt, J. E. Melzer, J. A. Harrington, and O. Mitrofanov, "Terahertz wave transmission in flexible polystyrene-lined hollow metallic waveguides for the 2.5-5 THz band," Opt. Express **21**(20), 23748–23755 (2013) (in English).
[116]G. N. Hou *et al.*, "Fabrication of Ag/PP terahertz hollow waveguide by vacuum evaporation method and transmission performance investigations," Opt. Mater. **147**, 114710 (2024) (in English).
[117]R. Mendis and D. Grischkowsky, "Plastic ribbon THz waveguides," J. Appl. Phys. **88**(7), 4449–4451 (2000).
[118]M. Nagel, A. Marchewka, and H. Kurz, "Low-index discontinuity terahertz waveguides," Opt. Express **14**(21), 9944–9954 (2006).
[119]S. Atakaramians, S. Afshar V, B. M. Fischer, D. Abbott, and T. M. Monro, "Porous fibers: A novel approach to low loss THz waveguides," Opt. Express **16**(12), 8845–8854 (2008).
[120]M. Rozé, B. Ung, A. Mazhorova, M. Walther, and M. Skorobogatiy, "Suspended core subwavelength fibers towards practical designs for low-loss terahertz guidance," Opt. Express **19**(10), 9127–9138 (2011).
[121]S. Atakaramians, S. Afshar V, H. Ebendorff-Heidepriem, M. Nagel, B. M. Fischer *et al.*, "THz porous fibers: Design, fabrication and experimental characterization," Opt. Express **17**(16), 14053–14062 (2009).
[122]W. Talataisong *et al.*, "Singlemoded THz guidance in bendable TOPAS suspended-core fiber directly drawn from a 3D printer," Sci. Rep. **10**(1), 11045 (2020).
[123]G. Xu, K. Nallappan, Y. Cao, and M. Skorobogatiy, "Infinity additive manufacturing of continuous microstructured fiber links for THz communications," Sci. Rep. **12**(1), 4551 (2022).
[124]G. Xu and M. Skorobogatiy, "Continuous fabrication of polarization maintaining fibers via an annealing improved infinity additive manufacturing technique for THz communications," Opt. Express **31**(8), 12894 (2023).
[125]H. Bao, K. Nielsen, H. K. Rasmussen, P. U. Jepsen, and O. Bang, "Fabrication and characterization of porous-core honeycomb bandgap THz fibers," Opt. Express **20**(28), 29507–29517 (2012).
[126]S. Jamison, R. McGowan, and D. Grischkowsky, "Single-mode waveguide propagation and reshaping of sub-ps terahertz pulses in sapphire fibers," Appl. Phys. Lett. **76**(15), 1987–1989 (2000).

[127]L.-J. Chen, H.-W. Chen, T.-F. Kao, J.-Y. Lu, and C.-K. Sun, "Low-loss subwavelength plastic fiber for terahertz waveguiding," Opt. Lett. **31**(3), 308–310 (2006).
[128]A. Hassani, A. Dupuis, and M. Skorobogatiy, "Low loss porous terahertz fibers containing multiple subwavelength holes," Appl. Phys. Lett. **92**, 071101 (2008).
[129]A. Hassani, A. Dupuis, and M. Skorobogatiy, "Porous polymer fibers for low-loss Terahertz guiding," Opt. Express **16**(9), 6340–6351 (2008).
[130]A. Dupuis, A. Mazhorova, F. Désévédavy, M. Rozé, and M. Skorobogatiy, "Spectral characterization of porous dielectric subwavelength THz fibers fabricated using a microstructured molding technique," Opt. Express **18**(13), 13813 (2010).
[131]Y. S. Lee *et al.*, "Low-loss polytetrafluoroethylene hexagonal porous fiber for terahertz pulse transmission in the 6G mobile communication window," IEEE Trans. Microwave Theory Tech. **69**(11), 4623–4630 (2021).
[132]T. Ma, A. Markov, L. Wang, and M. Skorobogatiy, "Graded index porous optical fibers—Dispersion management in terahertz range," Opt. Express **23**(6), 7856 (2015).
[133]S. Atakaramians, S. Afshar V, B. M. Fischer, D. Abbott, and T. M. Monro, "Low loss, low dispersion and highly birefringent terahertz porous fibers," Opt. Commun. **282**(1), 36–38 (2009).
[134]K. Nielsen, H. K. Rasmussen, P. U. Jepsen, and O. Bang, "Porous-core honeycomb bandgap THz fiber," Opt. Lett. **36**(5), 666–668 (2011).
[135]S. F. Kaijage, Z. Ouyang, and X. Jin, "Porous-core photonic crystal fiber for low loss terahertz wave guiding," IEEE Photonics Technol. Lett. **25**(15), 1454–1457 (2013).
[136]R. Islam, M. S. Habib, G. K. M. Hasanuzzaman, R. Ahmad, S. Rana, and S. F. Kaijage, "Extremely high-birefringent asymmetric slotted-core photonic crystal fiber in THz regime," IEEE Photonics Technol. Lett. **27**(21), 2222–2225 (2015).
[137]S. Ali, N. Ahmed, S. Aljunid, and B. Ahmad, "Hybrid porous core low loss dispersion flattened fiber for THz propagation," Photonics Nanostruct.-Fundam. Appl. **22**, 18–23 (2016).
[138]M. R. Hasan, M. A. Islam, and A. A. Rifat, "A single mode porous-core square lattice photonic crystal fiber for THz wave propagation," J. Eur. Opt. Soc. **12**(1), 15–18 (2016).
[139]R. Islam, M. S. Habib, G. Hasanuzzaman, S. Rana, M. A. Sadath, and C. Markos, "A novel low-loss diamond-core porous fiber for polarization maintaining terahertz transmission," IEEE Photonics Technol. Lett. **28**(14), 1537–1540 (2016).
[140]J. Liang, L. Ren, N. Chen, and C. Zhou, "Broadband, low-loss, dispersion flattened porous-core photonic bandgap fiber for terahertz (THz)-wave propagation," Opt. Commun. **295**, 257–261 (2013).
[141]Y.-F. Zhu, M.-Y. Chen, H. Wang, H.-B. Yao, Y.-K. Zhang, and J.-C. Yang, "Design and analysis of a low-loss suspended core terahertz fiber and its application to polarization splitter," IEEE Photonics J. **5**(6), 7101410 (2013).
[142]J. Fan, Y. Li, M. Hu, L. Chai, and C. Wang, "Design of broadband porous-core bandgap terahertz fibers," IEEE Photonics Technol. Lett. **28**(10), 1096–1099 (2016).
[143]M. T. Ahammed *et al.*, "Design of porous core fiber for terahertz regime using Zeonex," in *2021 4th International Conference on Computing and Communications Technologies (ICCCT)* (IEEE, 2021), pp. 538–543.
[144]M. S. Islam, J. Sultana, J. Atai, D. Abbott, S. Rana, and M. R. Islam, "Ultra low-loss hybrid core porous fiber for broadband applications," Appl. Opt. **56**(4), 1232–1237 (2017).
[145]S. Mei *et al.*, "A porous core Zeonex THz fiber with low loss and small dispersion," Opt. Fiber Technol. **69**, 102834 (2022).
[146]K. Nielsen, H. K. Rasmussen, A. J. Adam, P. C. M. Planken, O. Bang, and P. U. Jepsen, "Bendable, low-loss Topas fibers for the terahertz frequency range," Opt. Express **17**(10), 8592–8601 (2009).
[147]K. Wang and D. M. Mittleman, "Metal wires for terahertz wave guiding," Nature **432**(7015), 376–379 (2004).
[148]S. A. Maier, S. R. Andrews, L. Martín-Moreno, and F. J. García-Vidal, "Terahertz surface plasmon-polariton propagation and focusing on periodically corrugated metal wires," Phys. Rev. Lett. **97**(17), 176805 (2006).
[149]J. Anthony, R. Leonhardt, and A. Argyros, "Hybrid hollow core fibers with embedded wires as THz waveguides," Opt. Express **21**(3), 2903–2912 (2013) (in English).
[150]M. Mbonye, R. Mendis, and D. M. Mittleman, "A terahertz two-wire waveguide with low bending loss," Appl. Phys. Lett. **95**(23), 233506 (2009).
[151]S. Atakaramians *et al.*, "Fiber-drawn metamaterial for THz waveguiding and imaging," J. Infrared, Millimeter, Terahertz Waves **38**(9), 1162–1178 (2017) (in English).
[152]N. Yudasari, J. Anthony, and R. Leonhardt, "Terahertz pulse propagation in 3D-printed waveguide with metal wires component," Opt. Express **22**(21), 26042–26054 (2014) (in English).
[153]D. B. Tian *et al.*, "Dual cylindrical metallic grating-cladding polymer hollow waveguide for terahertz transmission with low loss," Appl. Phys. Lett. **97**(13), 133502 (2010) (in English).
[154]O. T. Naman *et al.*, "Indefinite media based on wire array metamaterials for the THz and Mid-IR," Adv. Opt. Mater. **1**(12), 971–977 (2013) (in English).
[155]A. Markov, H. Guerboukha, A. Argyros, and M. Skorobogatiy, "A complementary study to 'Hybrid hollow core fibers with embedded wires as THz waveguides' and 'Two-wire terahertz fibers with porous dielectric support:' comment," Opt. Express **21**(23), 27802–27803 (2013) (in English).
[156]H. S. Li *et al.*, "Flexible single-mode hollow-core terahertz fiber with metamaterial cladding," Optica **3**(9), 941–947 (2016) (in English).
[157]S. Atakaramians, A. Argyros, S. C. Fleming, and B. T. Kuhlmey, "Hollow-core uniaxial metamaterial clad fibers with dispersive metamaterials," J. Opt. Soc. Am. B **30**(4), 851–867 (2013) (in English).
[158]S. Atakaramians, A. Argyros, S. C. Fleming, and B. T. Kuhlmey, "Hollow-core waveguides with uniaxial metamaterial cladding: Modal equations and guidance conditions," J. Opt. Soc. Am. B **29**(9), 2462–2477 (2012) (in English).
[159]P. Shekhar, J. Atkinson, and Z. Jacob, "Hyperbolic metamaterials: Fundamentals and applications," Nano Convergence **1**(1), 14 (2014) (in English).
[160]S. Jahani and Z. Jacob, "Transparent subdiffraction optics: Nanoscale light confinement without metal," Optica **1**(2), 96–100 (2014) (in English).
[161]M. Yan and N. A. Mortensen, "Hollow-core infrared fiber incorporating metal-wire metamaterial," Opt. Express **17**(17), 14851–14864 (2009) (in English).
[162]A. Tuniz, R. Lwin, A. Argyros, S. C. Fleming, and B. T. Kuhlmey, "Fabricating metamaterials using the fiber drawing method," J. Visualized Exp. **68**, e4299 (2012).
[163]H. S. Li, G. B. Ren, S. Atakaramians, B. T. Kuhlmey, and S. S. Jian, "Linearly polarized single TM mode terahertz waveguide," Opt. Lett. **41**(17), 4004–4007 (2016) (in English).
[164]T. Pandey, M. Reza, and A. K. Paul, "Aluminum coated hollow-core fiber for single mode operation in the terahertz spectrum," OSA Continuum **4**, 1981 (2021).
[165]J. Sultana *et al.*, "Terahertz hollow core antiresonant fiber with metamaterial cladding," Fibers **8**(2), 14 (2020).
[166]T.-I. Jeon and D. Grischkowsky, "THz Zenneck surface wave (THz surface plasmon) propagation on a metal sheet," Appl. Phys. Lett. **88**, 061113 (2006).
[167]K. Wang and D. M. Mittleman, "Dispersion of surface plasmon polaritons on metal wires in the terahertz frequency range," Phys. Rev. Lett. **96**(15), 157401 (2006).
[168]T.-I. Jeon, J. Zhang, and D. Grischkowsky, "THz Sommerfeld wave propagation on a single metal wire," Appl. Phys. Lett. **86**, 161904 (2005).
[169]V. Astley, J. Scheiman, R. Mendis, and D. M. Mittleman, "Bending and coupling losses in terahertz wire waveguides," Opt. Lett. **35**(4), 553–555 (2010).
[170]N. C. J. van der Valk and P. C. M. Planken, "Effect of a dielectric coating on terahertz surface plasmon polaritons on metal wires," Appl. Phys. Lett. **87**(7), 071106 (2005).
[171]G. Goubau, "Surface waves and their application to transmission lines," J. Appl. Phys. **21**(11), 1119–1128 (1950).
[172]A. I. Fernandez-Dominguez, L. Martin-Moreno, F. J. Garcia-Vidal, S. R. Andrews, and S. A. Maier, "Spoof surface plasmon polariton modes propagating along periodically corrugated wires," IEEE J. Sel. Top. Quantum Electron. **14**(6), 1515–1521 (2008).
[173]P. Tannouri, M. Peccianti, P. L. Lavertu, F. Vidal, and R. Morandotti, "Quasi-TEM mode propagation in twin-wire THz waveguides (Invited Paper)," Chin. Opt. Lett. **9**(11), 110013–110016 (2011).
[174]H. Pahlevaninezhad and T. E. Darcie, "Coupling of terahertz waves to a two-wire waveguide," Opt. Express **18**(22), 22614–22624 (2010).

[175]H. Pahlevaninezhad, T. E. Darcie, and B. Heshmat, "Two-wire waveguide for terahertz," Opt. Express **18**(7), 7415–7420 (2010).
[176]D. Teng, Q. Cao, S. Li, and H. Gao, "Tapered dual elliptical plasmon waveguides as highly efficient terahertz connectors between approximate plate waveguides and two-wire waveguides," J. Opt. Soc. Am. A **31**(2), 268–273 (2014).
[177]H. Gao, Q. Cao, D. Teng, M. Zhu, and K. Wang, "Perturbative solution for terahertz two-wire metallic waveguides with different radii," Opt. Express **23**(21), 27457–27473 (2015).
[178]R. Leonhardt, J. Anthony, and A. Argyros, "THz propagation in hybrid hollow core fibers with metal wires inclusion," in *2013 Conference on Lasers and Electro-Optics - International Quantum Electronics Conference*, paper CC_P_8 (2013).
[179]A. Markov and M. Skorobogatiy, "Two-wire terahertz fibers with porous dielectric support," Opt. Express **21**(10), 12728 (2013).
[180]S. Pandey, B. Gupta, and A. Nahata, "Terahertz plasmonic waveguides created via 3D printing," Opt. Express **21**(21), 24422 (2013).
[181]T. Ma, K. Nallapan, H. Guerboukha, and M. Skorobogatiy, "Analog signal processing in the terahertz communication links using waveguide Bragg gratings: Example of dispersion compensation," Opt. Express **25**(10), 11009–11026 (2017).
[182]C. H. Brodie *et al.*, "Comprehensive study of 3D printing materials over the terahertz regime: Absorption coefficient and refractive index characterizations," Opt. Mater. Express **12**(9), 3379–3402 (2022) (in English).
[183]K. Nallappan *et al.*, "Terahertz waveguides for next generation communication network: Needs, challenges and perspectives," in *Next Generation Wireless Terahertz Communication Networks* (CRC Press, 2021), pp. 379–410.
[184]H.-J. Song, "Packages for terahertz electronics," Proc. IEEE **105**(6), 1121–1138 (2017).
[185]Y. Dong, V. Zhurbenko, P. J. Hanberg, and T. K. Johansen, "A D-band rectangular waveguide-to-coplanar waveguide transition using wire bonding probe," J. Infrared, Millimeter, Terahertz Waves **40**, 63–79 (2019).
[186]P. Stärke, C. Carta, and F. Ellinger, "Direct chip-to-waveguide transition realized with wire bonding for 140–220 GHz G-band," IEEE Trans. Terahertz Sci. Technol. **10**(3), 302–308 (2020).
[187]X. Yu *et al.*, "Terahertz fibre transmission link using resonant tunnelling diodes integrated with photonic-crystal waveguides," Electron. Lett. **55**(7), 398–400 (2019).
[188]R. Koala, K. Iyoda, W. Gao, Y. Matsuura, M. Fujita, and T. Nagatsuma, "Terahertz fiber link using dielectric silicon waveguide interface," Opt. Express **31**(5), 7351–7362 (2023).
[189]J. Ding *et al.*, "352-Gbit/s single line rate THz wired transmission based on PS-4096QAM employing hollow-core fiber," Digital Commun. Networks **9**(3), 717–722 (2023).
[190]J. Ma, M. Weidenbach, R. Guo, M. Koch, and D. Mittleman, "Communications with THz waves: Switching data between two waveguides," J. Infrared, Millimeter, Terahertz Waves **38**, 1316–1320 (2017).
[191]Y. Cao, K. Nallappan, G. Xu, and M. Skorobogatiy, "Add drop multiplexers for terahertz communications using two-wire waveguide-based plasmonic circuits," Nat. Commun. **13**(1), 4090 (2022).
[192]J. Dong *et al.*, "Versatile metal-wire waveguides for broadband terahertz signal processing and multiplexing," Nat. Commun. **13**(1), 741 (2022).
[193]J. Yu, X. Li, X. Tang, H. Zhang, N. Chi, and Y. Shi, "High-speed signal transmission at W-band over dielectric-coated metallic hollow fiber," IEEE Trans. Microwave Theory Tech. **63**(6), 1836–1842 (2015).
[194]M. De Wit, Y. Zhang, and P. Reynaert, "Analysis and design of a foam-cladded PMF link with phase tuning in 28-nm CMOS," IEEE J. Solid-State Circuits **54**(7), 1960–1969 (2019).
[195]M. Sawaby, N. Dolatsha, B. Grave, C. Chen, and A. Arbabian, "A fully packaged 130-GHz QPSK transmitter with an integrated PRBS generator," IEEE Solid-State Circuits Lett. **1**(7), 166–169 (2018).
[196]J. Vaes, K. Dens, G. Ducournau, and P. Reynaert, "Plastic microwave fibers at millimeter-wave and THz frequencies as a low cost data link," in *2021 IEEE MTT-S International Microwave Symposium (IMS)* (IEEE, 2021), pp. 589–591.
[197]K. Nallappan, H. Guerboukha, Y. Cao, C. Nerguizian, and M. Skorobogatiy, "Experimental demonstration of 5 Gbps data transmission using long subwavelength fiber at 140 GHz," in *2019 IEEE Radio and Wireless Symposium (RWS)* (IEEE, 2019), pp. 1–4.
[198]C. E. Shannon, "A mathematical theory of communication," Bell Syst. Tech. J. **27**(3), 379–423 (1948).
[199]M. Zhu, J. Zhang, J. Yu, and X. You, "Demonstration of record-high 352-Gbps terahertz wired transmission over hollow-core fiber at 325 GHz," Sci. China Inf. Sci. **65**(2), 127301 (2022).
[200]S. F. Zhou, L. Reekie, H. P. Chan, Y. T. Chow, P. S. Chung, and K. Man Luk, "Characterization and modeling of Bragg gratings written in polymer fiber for use as filters in the THz region," Opt. Express **20**(9), 9564–9571 (2012).
[201]M. Ghazialsharif *et al.*, "Engineering topological interface states in metal-wire waveguides for broadband terahertz signal processing," Nanophotonics **13**(10), 1929–1937 (2024).
[202]G. Yan, A. Markov, Y. Chinifooroshan, S. M. Tripathi, W. J. Bock, and M. Skorobogatiy, "Low-loss terahertz waveguide Bragg grating using a two-wire waveguide and a paper grating," Opt. Lett. **38**(16), 3089–3092 (2013).
[203]M. Weidenbach *et al.*, "3D printed dielectric rectangular waveguides, splitters and couplers for 120 GHz," Opt. Express **24**(25), 28968–28976 (2016).
[204]H. Zhao, B. Quan, X. Wang, C. Gu, J. Li, and Y. Zhang, "Demonstration of orbital angular momentum multiplexing and demultiplexing based on a metasurface in the terahertz band," ACS Photonics **5**(5), 1726–1732 (2017).
[205]W. Liu *et al.*, "Multifunctional all-dielectric metasurfaces for terahertz multiplexing," Adv. Opt. Mater. **9**(19), 2100506 (2021).
[206]D. Headland, W. Withayachumnankul, M. Fujita, and T. Nagatsuma, "Gratingless integrated tunneling multiplexer for terahertz waves," Optica **8**(5), 621–629 (2021).
[207]N. J. Karl, R. W. McKinney, Y. Monnai, R. Mendis, and D. M. Mittleman, "Frequency-division multiplexing in the terahertz range using a leaky-wave antenna," Nat. Photonics **9**(11), 717–720 (2015).
[208]L. Jie, H. Li, Y. Liu, J. Wang, G. Ren, and L. Pei, "Terahertz multidimensional-multiplexing and refractive-index-sensing integrated device," Acta Opt. Sin. **44**(8), 0823001 (2024).
[209]M. K. Mridha *et al.*, "Active terahertz two-wire waveguides," Opt. Express **22**(19), 22340–22348 (2014).
[210]D. Wang, Y. Zhang, Y. Qi, J. Tian, S. Yue, and T. Ma, "Tunable surface plasmon resonance sensor based on graphene-coated photonic crystal fiber in terahertz," Appl. Opt. **61**(22), 6664–6670 (2022).
[211]K. Ito, T. Katagiri, and Y. Matsuura, "Analysis of transmission properties of terahertz hollow-core optical fiber by using time-domain spectroscopy and application for remote spectroscopy," J. Opt. Soc. Am. B **34**(1), 60–65 (2017).
[212]Y. Matsuura, T. Suzuki, and T. Katagiri, "Terahertz gas sensing based on time-domain-spectroscopy using a hollow-optical fiber gas cell," Proc. SPIE **10488**, 1048808 (2018).
[213]M. S. Islam *et al.*, "Single-step tabletop fabrication for low-attenuation terahertz special optical fibers," Adv. Photonics Res. **2**(12), 2100165 (2021).
[214]M. Walther, M. R. Freeman, and F. A. Hegmann, "Metal-wire terahertz time-domain spectroscopy," Appl. Phys. Lett. **87**(26), 261107 (2005).
[215]J.-Y. Lu, B. You, J.-Y. Wang, S.-S. Jhuo, T.-Y. Hung, and C.-P. Yu, "Volatile gas sensing through terahertz pipe waveguide," Sensors **20**(21), 6268 (2020).
[216]G. Yan, A. Markov, Y. Chinifooroshan, S. M. Tripathi, W. J. Bock, and M. Skorobogatiy, "Resonant THz sensor for paper quality monitoring using THz fiber Bragg gratings," Opt. Lett. **38**(13), 2200 (2013).
[217]B. You, J.-Y. Lu, T.-A. Liu, J.-L. Peng, and C.-L. Pan, "Subwavelength plastic wire terahertz time-domain spectroscopy," Appl. Phys. Lett. **96**(5), 051105 (2010).
[218]A. Mazhorova *et al.*, "Label-free bacteria detection using evanescent mode of a suspended core terahertz fiber," Opt. Express **20**(5), 5344–5355 (2012).
[219]B. Chen *et al.*, "Hollow-core metallic waveguide-based molecular sensing in terahertz to mid-infrared spectral range," IEEE Sens. J. **23**, 28923 (2023).
[220]B. You and J.-Y. Lu, "Remote and in situ sensing products in chemical reaction using a flexible terahertz pipe waveguide," Opt. Express **24**(16), 18013–18023 (2016).
[221]A. Hassani and M. Skorobogatiy, "Surface Plasmon Resonance-like integrated sensor at terahertz frequencies for gaseous analytes," Opt. Express **16**(25), 20206–20214 (2008).
[222]P. Padhy, P. K. Sahu, and R. Jha, "Metal wire waveguide based all plasmonic refractive index sensor for terahertz frequencies," Sens. Actuators, B **225**, 115–120 (2016).

[223]F. Fan *et al.*, "Terahertz transmission and sensing properties of microstructured PMMA tube waveguide," Opt. Express **23**(21), 27204–27212 (2015).
[224]Y. Cao, K. Nallappan, G. Xu, and M. Skorobogatiy, "Resonant gas sensing in the terahertz spectral range using two-wire phase-shifted waveguide Bragg gratings," Sensors **23**(20), 8527 (2023).
[225]H. Guerboukha, K. Nallappan, and M. Skorobogatiy, "Toward real-time terahertz imaging," Adv. Opt. Photonics **10**(4), 843–938 (2018) (in English).
[226]H. Sarieddeen, N. Saeed, T. Y. Al-Naffouri, and M. S. Alouini, "Next generation terahertz communications: A rendezvous of sensing, imaging, and localization," IEEE Commun. Mag. **58**(5), 69–75 (2020) (in English).
[227]J.-Y. Lu *et al.*, "Terahertz scanning imaging with a subwavelength plastic fiber," Appl. Phys. Lett. **92**, 084102 (2008).
[228]T. Yu, X. Zuo, W. W. Liu, and C. Gong, "0.1THz super-resolution imaging based on 3D printed confocal waveguides," Opt. Commun. **459**, 124896 (2020) (in English).
[229]M. He *et al.*, "Transmission and imaging characteristics of flexible gradually tapered waveguide at 0.3 THz," Opt. Express **29**(6), 8430–8440 (2021) (in English).
[230]A. Tuniz *et al.*, "Metamaterial fibres for subdiffraction imaging and focusing at terahertz frequencies over optically long distances," Nat. Commun. **4**, 2706 (2013) (in English).
[231]B. Chen *et al.*, "A low-loss hollow-core waveguide bundle for terahertz imaging under a cryogenic environment," ACS Photonics **11**, 3068 (2024) (in English).
[232]X. Y. Li *et al.*, "Super-resolution terahertz imaging based on a meta-waveguide," Opt. Lett. **49**(5), 1261–1264 (2024) (in English).
[233]D. Čibiraitė-Lukenskienė, K. Ikamas, T. Lisauskas, V. Krozer, H. G. Roskos, and A. Lisauskas, "Passive detection and imaging of human body radiation using an uncooled field-effect transistor-based THz detector," Sensors **20**(15), 4087 (2020).
[234]Y. Kajihara, T. Mizutani, and S. Komiyama, "Passive THz near-field imaging and its applications for engineering," Key Eng. Mater. **523-524**, 821–825 (2012).
[235]G. Hou *et al.*, "Robust integrated Ag/PP-PP/Ag hollow waveguide for low-loss and low-dispersion transmission of low-frequency terahertz waves: Design, fabrication and performances," J. Lightwave Technol. **43**, 299 (2025).
[236]D. Chen *et al.*, "Ultrahigh terahertz signal transmittance of PTFE@PPS nanocomposite foam designed for terahertz antennas," Ind. Eng. Chem. Res. **62**(38), 15511–15524 (2023).